Computational Neuroanatomy

Bruce Fischl

MGH ATHINOULA A. MARTINOS CENTER
Harvard Medical School

MIT CSAIL

Talk Outline

1. Cortical Analysis.
2. Subcortical Analysis.
3. Sources of distortion in MRI.
4. Linking micro structure to macro structure.

Talk Outline

1. Cortical Analysis.
2. Subcortical Analysis.
3. Sources of distortion in MRI.
4. Linking micro structure to macro structure.

Why Is a Model of the Cortical Surface Useful?

Local functional organization of cortex is largely 2-dimensional!

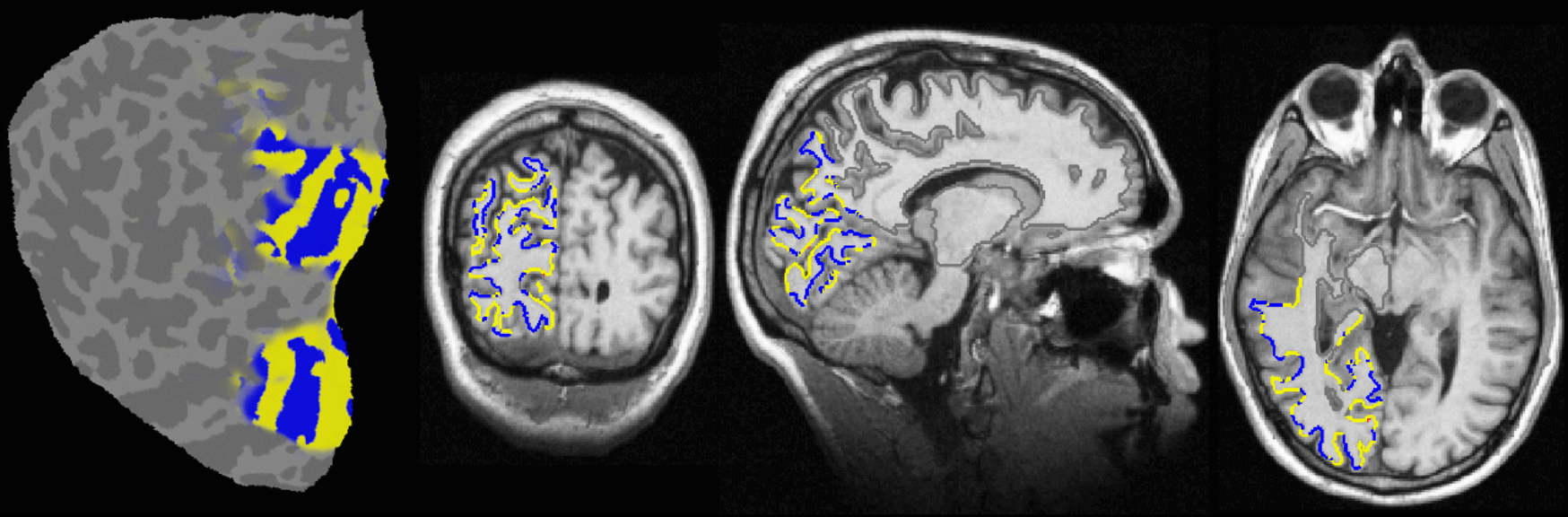

From (Sereno et al, 1995, Science).

Why Is Constructing a Model of The Cortical Surface Difficult?

The cortex is highly folded!

- Partial voluming.
- Subject motion.
- Susceptibility artifacts.
- Bias field.
- Tissue inhomogeneities.

Intensity of a tissue class varies as a function of spatial location

Sources of within-class intensity variation

- Partial voluming – a single voxel may contain more than one tissue type.
- Bias field – effective flip angle or sensitivity of receive coil may vary across space.
- Tissue inhomogeneities – even within tissue type (e.g. cortical gray matter), intrinsic properties such as T1, PD can vary (up to 20%).

T1 weighted MR volume

Assigning tissue classes to voxels can be difficult

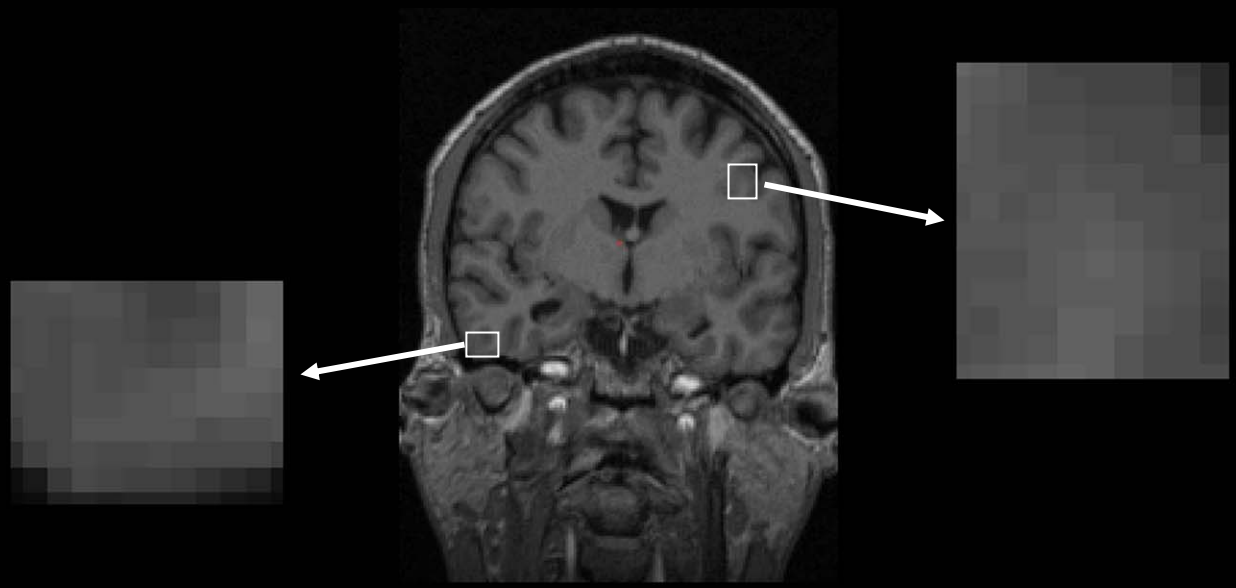

Which Surface to Reconstruct?

Pial surface **is ultimate goal, but pretty much impossible to directly generate a representation of from MRI images (many have tried!).**

Alternative: construct an interim representation of the interface between gray matter and white matter, and use it to infer the location of the true cortical surface (Dale and Sereno, 1993).

Skull Stripping and building of Boundary Element Models

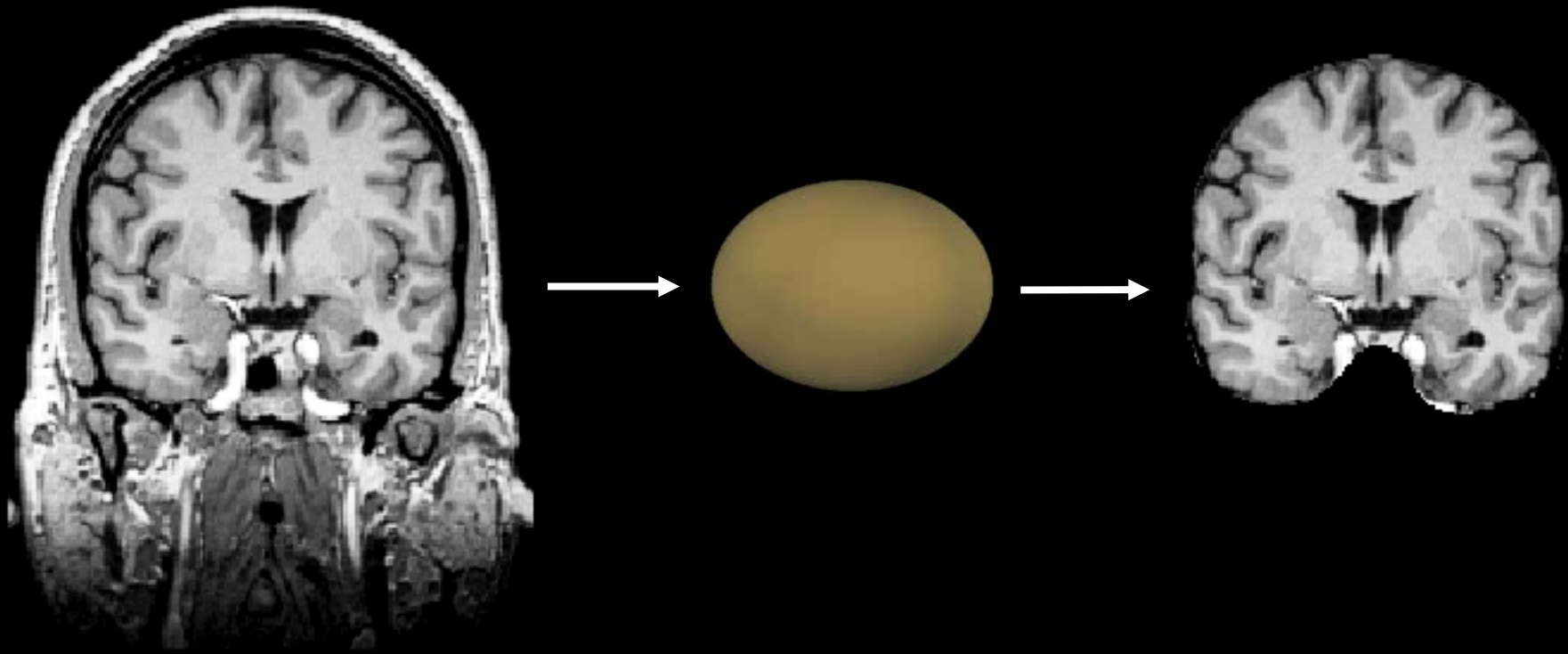

MRI Segmentation and Surface Reconstruction

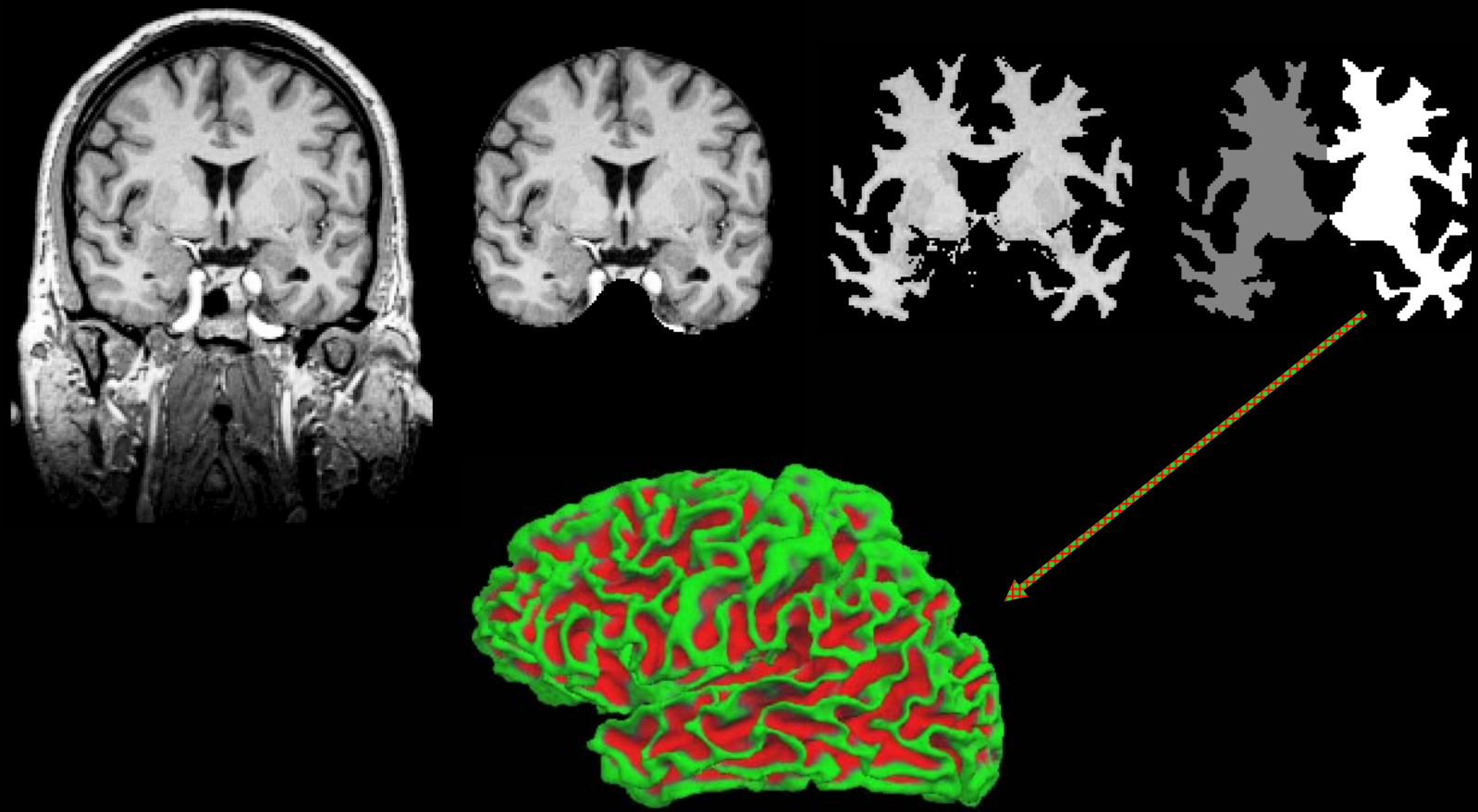

Topology Correction

The true topology of the cortical ribbon is that of a sheet (Euler number=1).

We would like the reconstructed gray/white boundary to have spherical topology (Euler number=2), but errors in the segmentation and non-cortical anatomical features of the white matter cause departures from spherical topology (“defects”).

Typical “Defects”

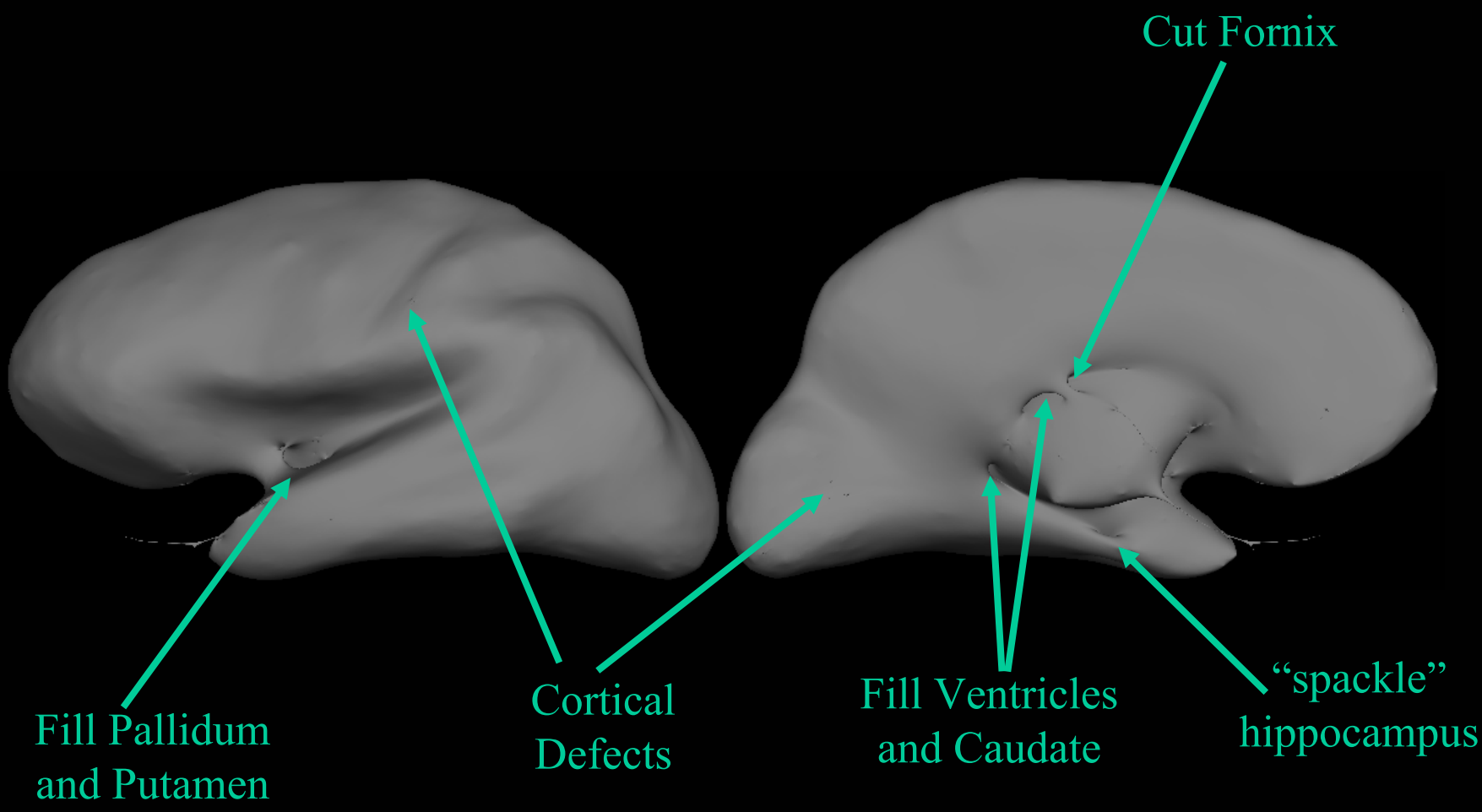

Topological Defects

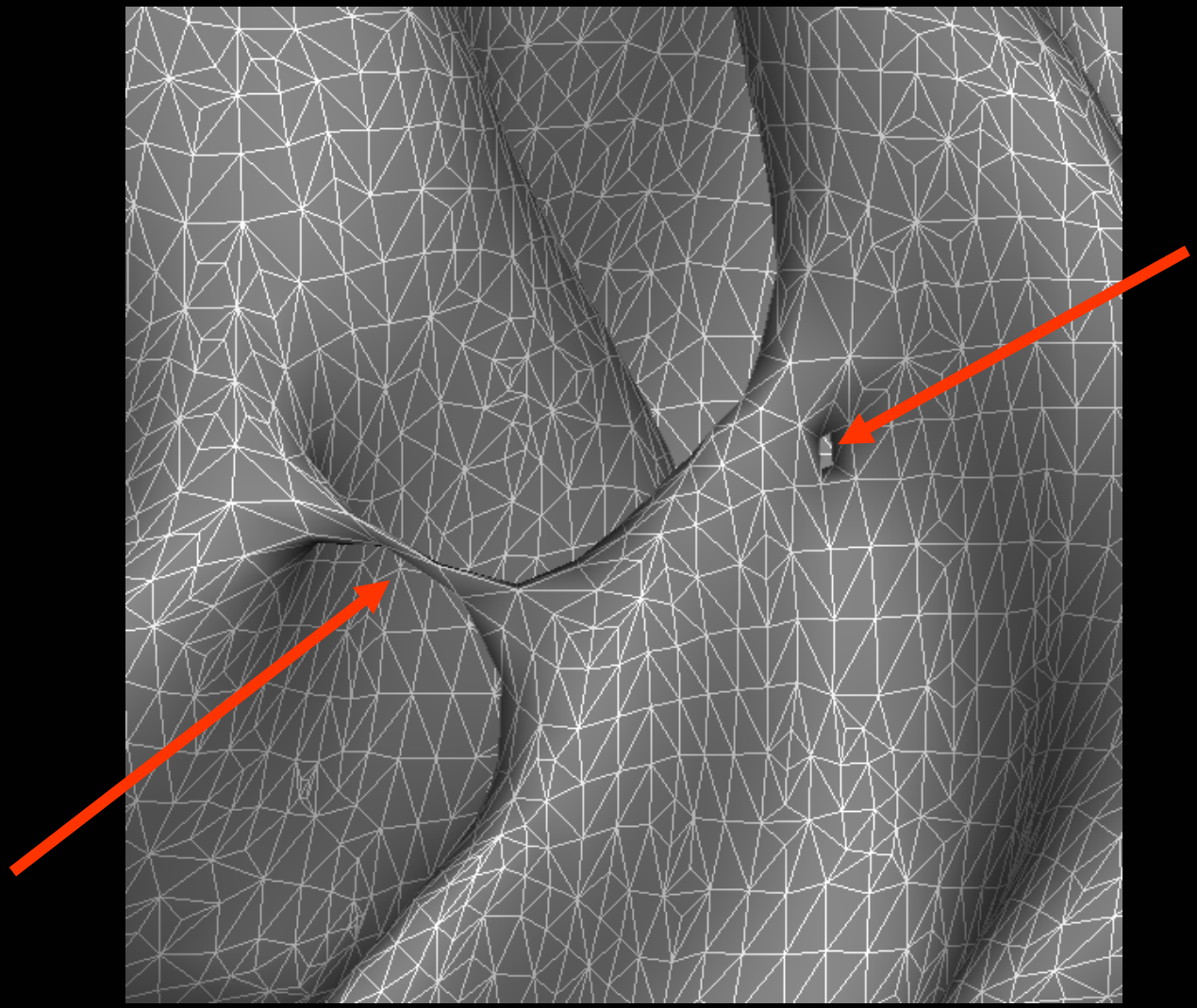

Standard method*: shrink wrapping

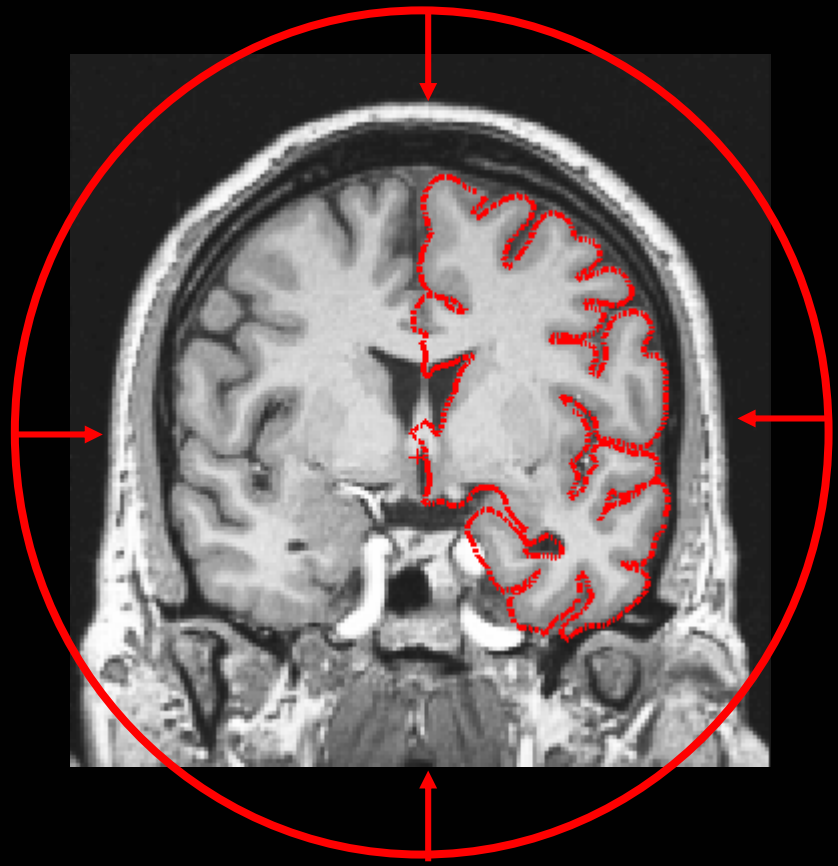

start with a surface S (e.g. sphere) of known topology find a mapping $M: S \mapsto C$ of it to the cortex *C* that doesn't change its topology (e.g. Davatzikos, 1996; Macdonald 2000)

*newer volumetric work (Shattuck and Leahy, 2001; Han et al., 2002)

How to maintain geometric accuracy?

Problems:

1. **The initial surface *S* is typically *much* smoother than the target surface *C*. The energy functionals for finding *M* are therefore highly non-convex.**

2. **Local errors that would have given rise to inaccurate segmentation if the topology were not constrained, can cause large scale geometric inaccuracies in the surfaces.**

What Surface Would a Shrink-Wrapping Algorithm Result in?

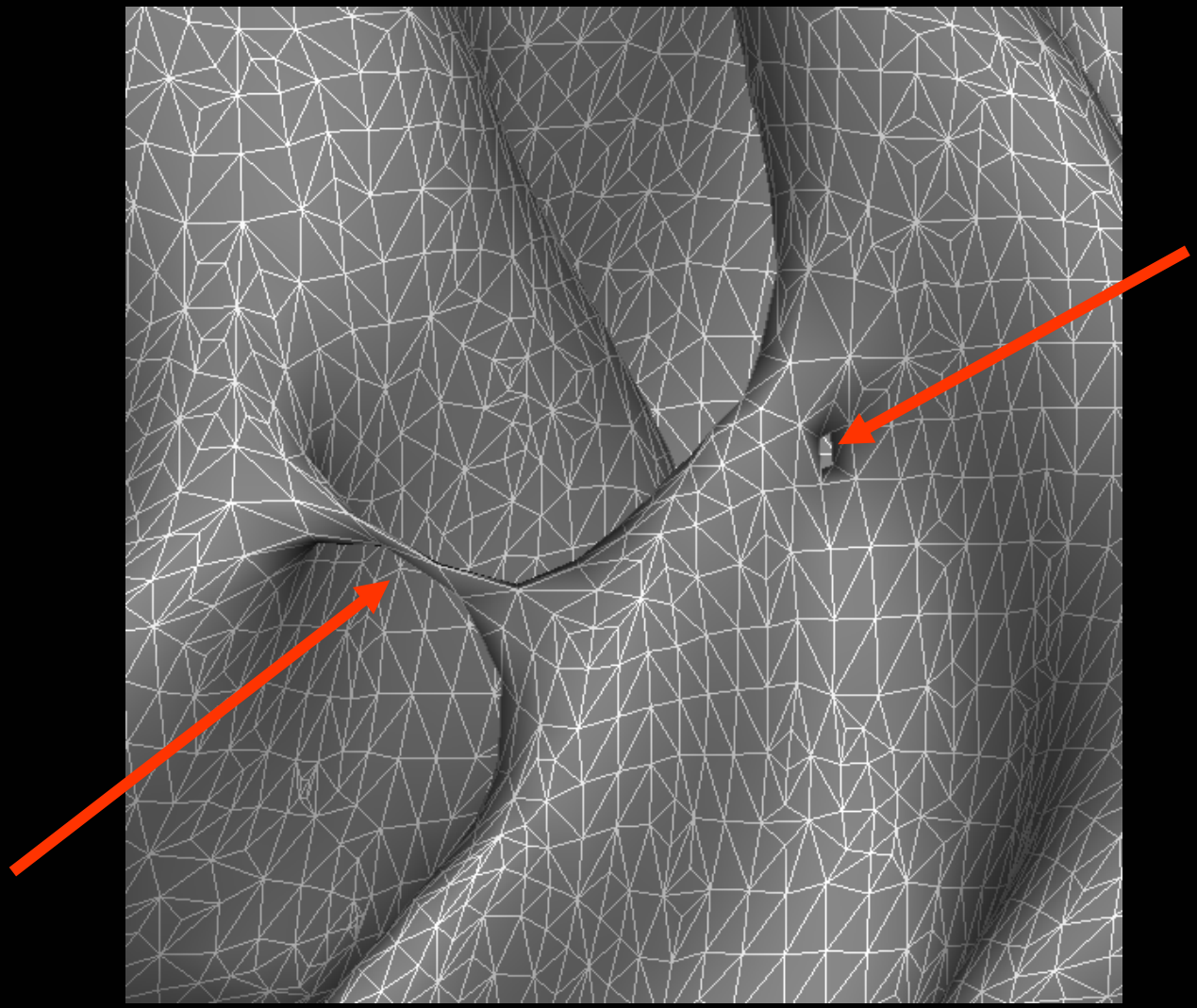

Solution: Manifold Surgery.

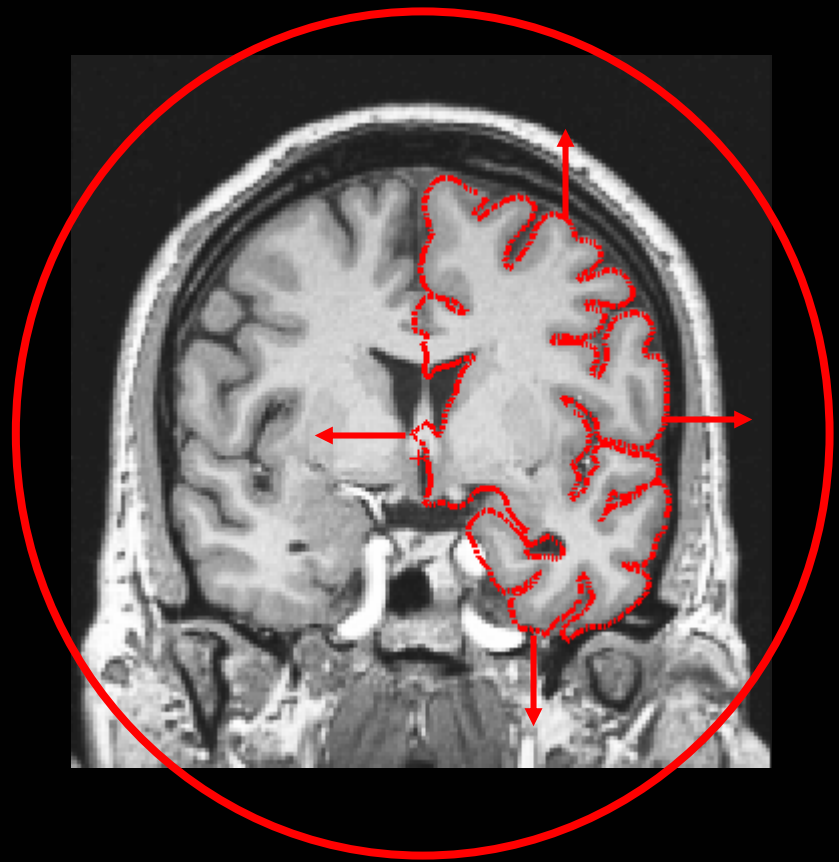

Generate *C*' and find a mapping M^{-1} from C' to *S* that is invertible over as much of *C* as possible. Noninvertible regions contain defects!

Manifold Surgery: Equations

Energy Functional: $$E = \sum_{i=1}^{F} \left(\frac{\log(1 + e^{-kR_i})}{k} \right)$$

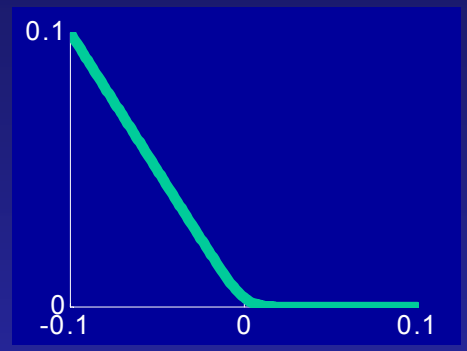

det(J)

R_i – jacobian at the i^{th} face in tessellation

F – number of faces in tessellation

k – positive real constant

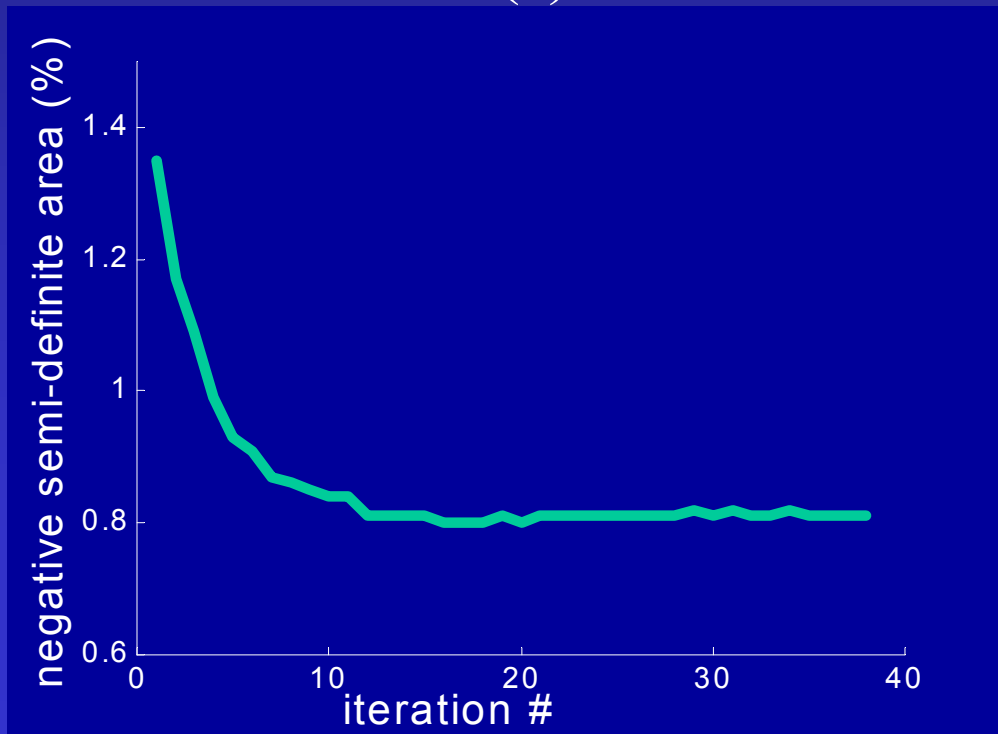

Detection of non-homeomorphic Regions

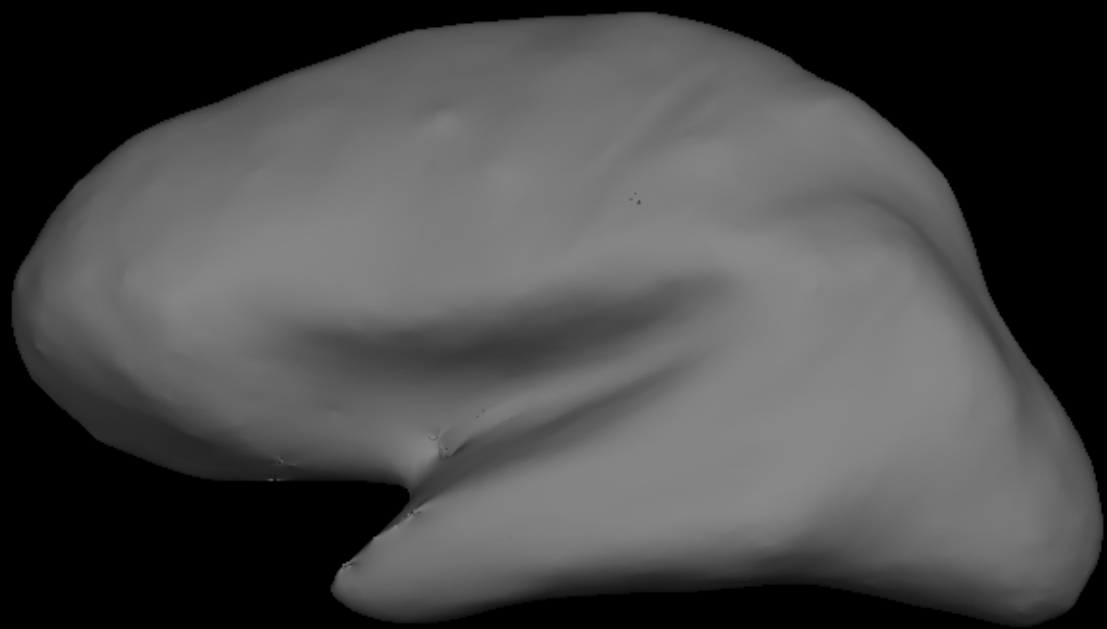

Detection of non-homeomorphic Regions

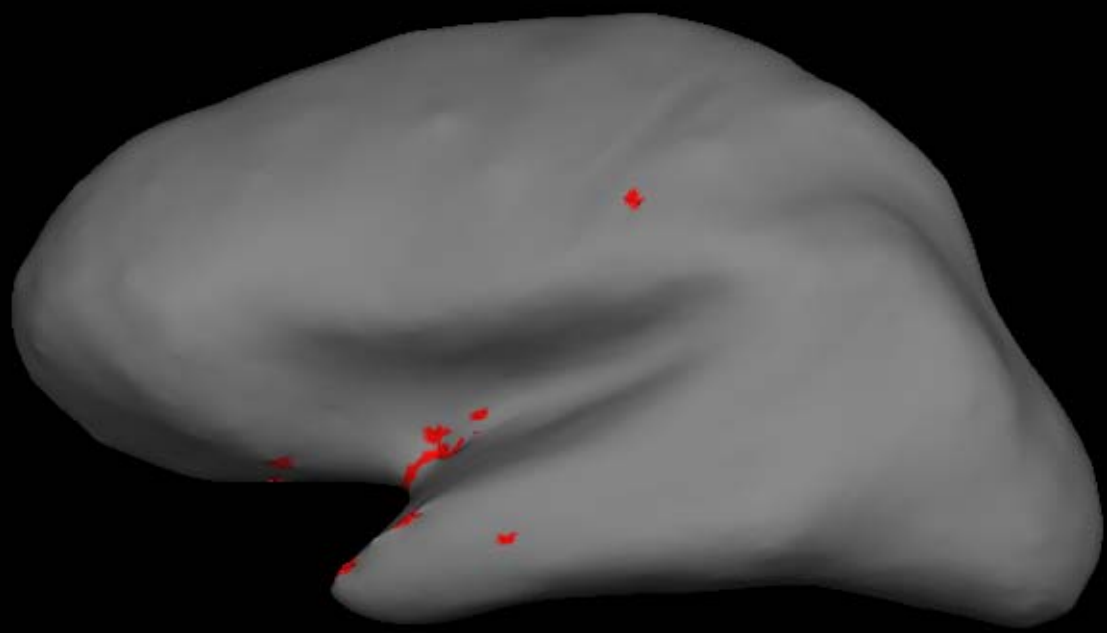

Detection of non-homeomorphic Regions

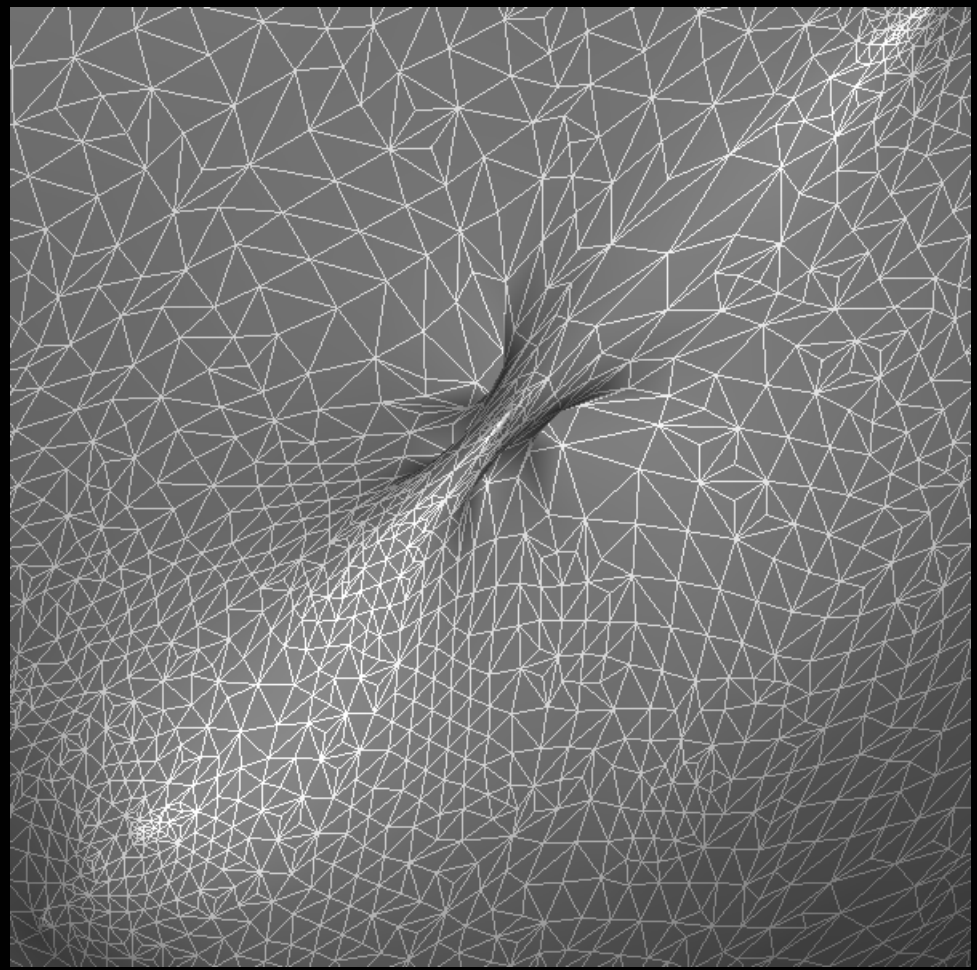

Detection of non-homeomorphic Regions

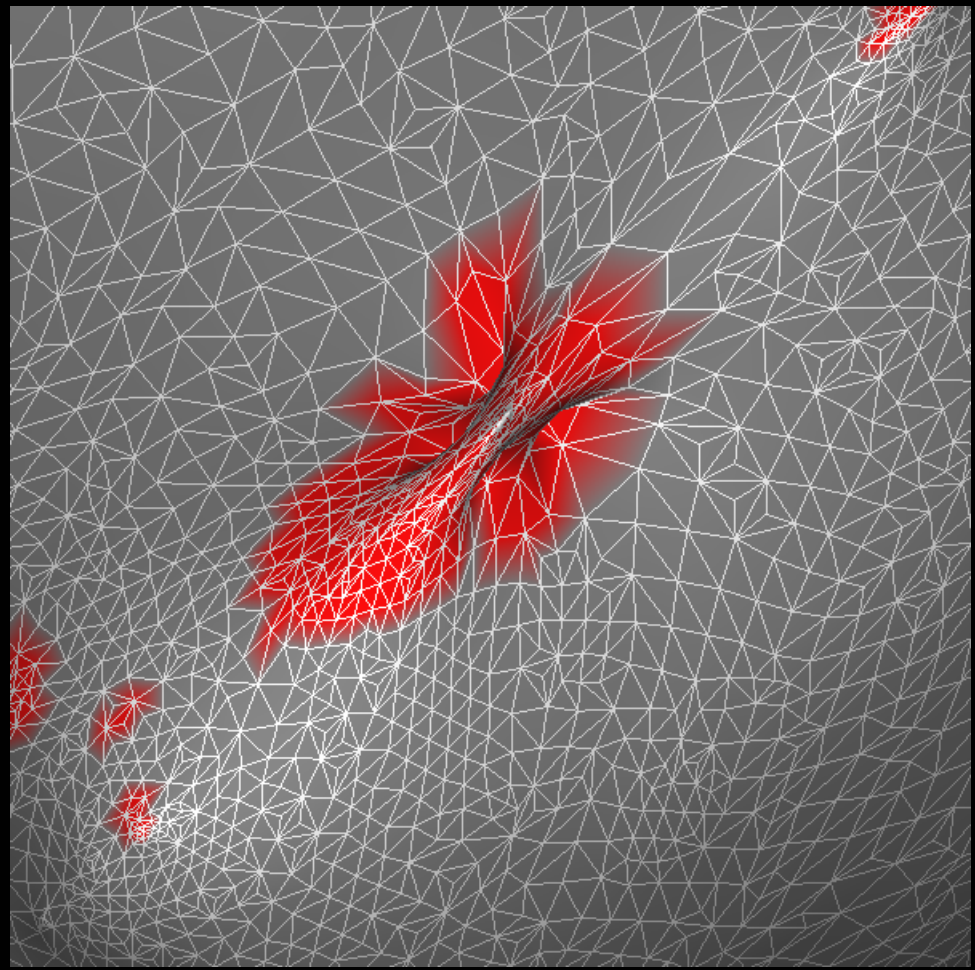

Manifold Surgery: Retessellation

1. Mark all triangles that have any edge overlapping any other edge in the tessellation.
2. Discard all faces and edges in marked triangles.
3. Sort all possible edges by image likelihood (they should go through MR values between gray and white).
4. Use a greedy retessellation algorithm: keep adding edges between all vertices in defects until no more can be added without causing an intersection with an existing edge ***on the sphere***.

(Florent Ségonne currently working on using genetic algorithm to evaluate different potential retessellations, but the space is huge!)

Manifold Surgery: Results

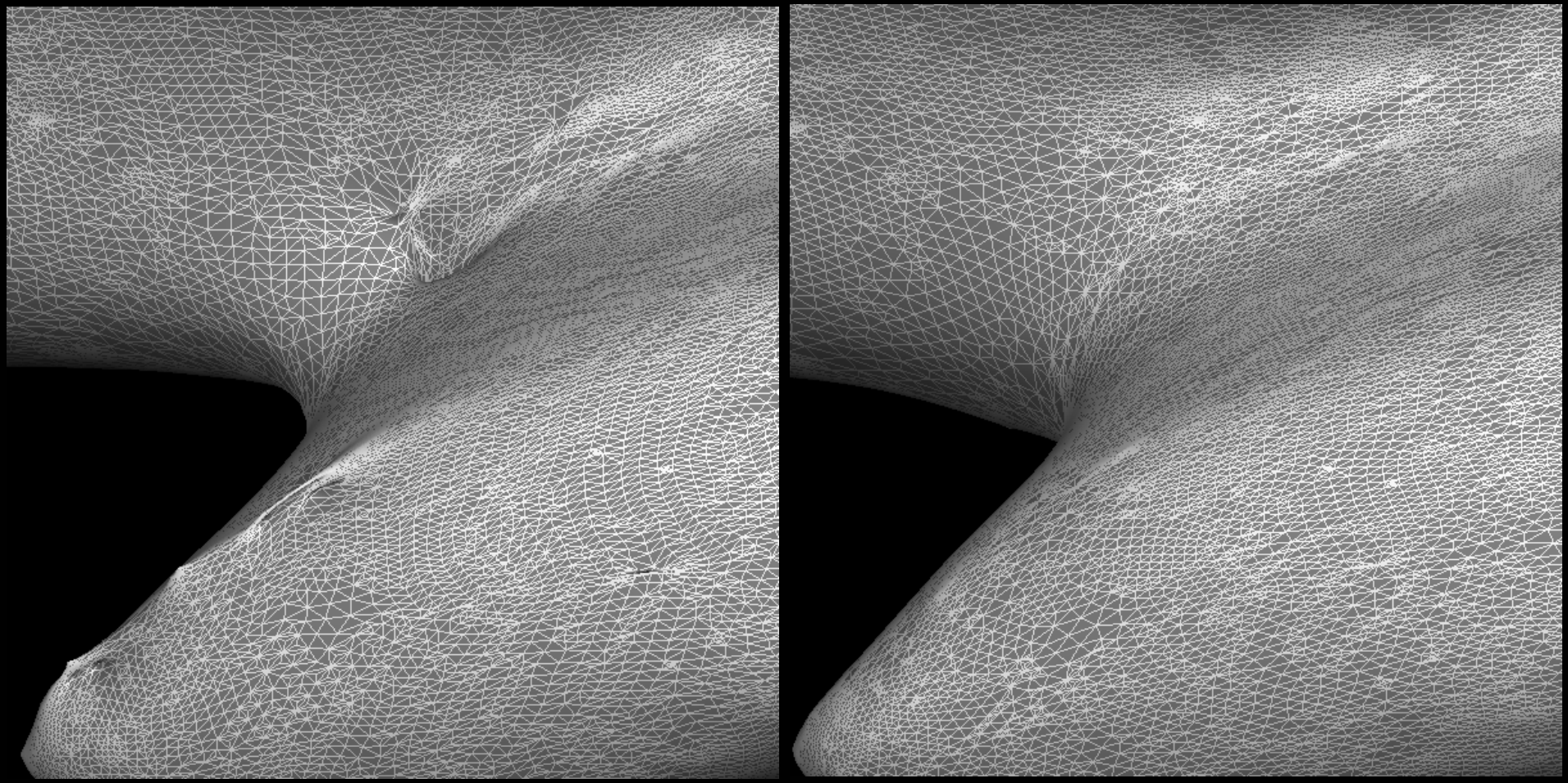

BEFORE

AFTER

Surface Inflation

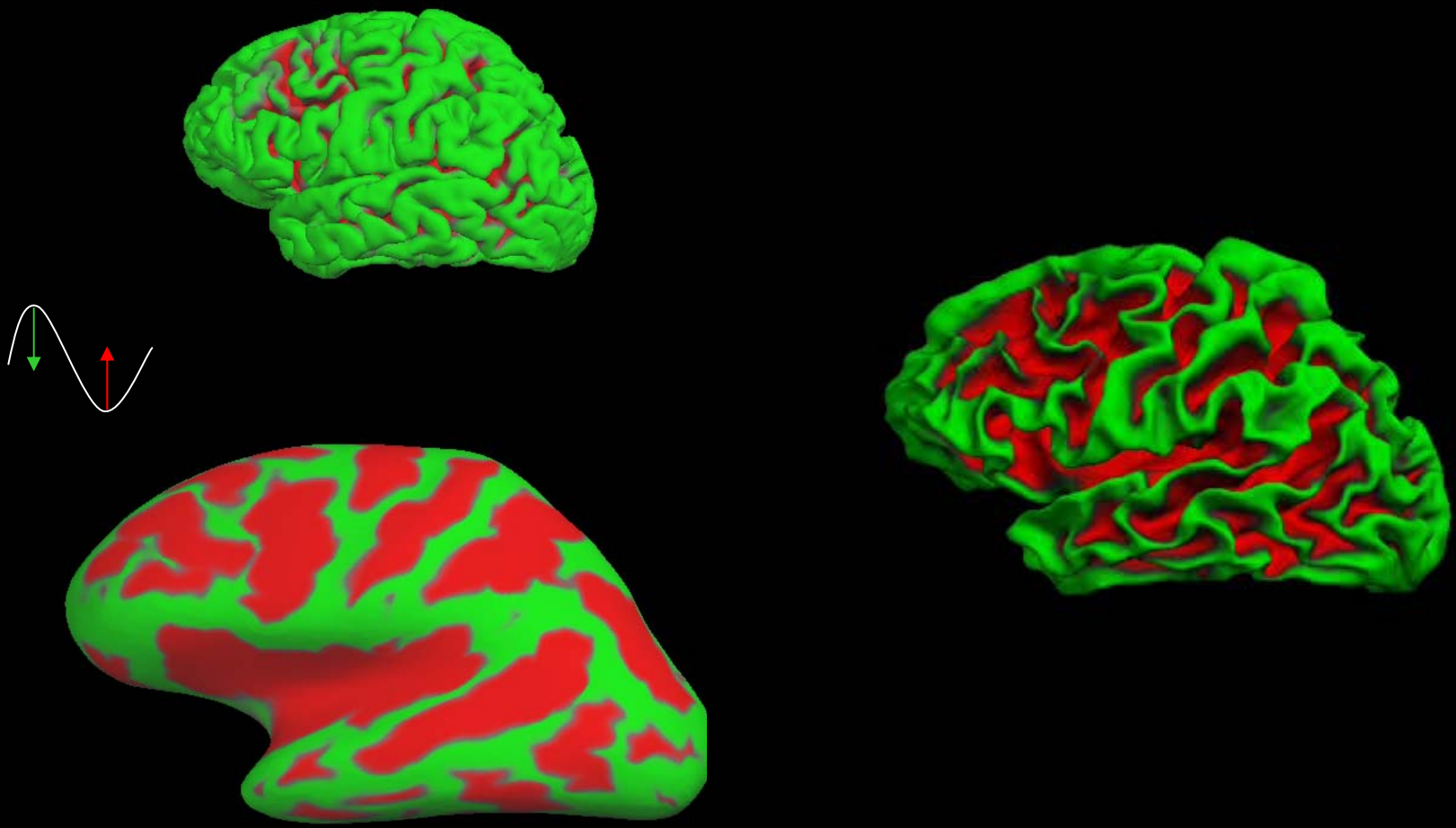

White matter and pial surfaces

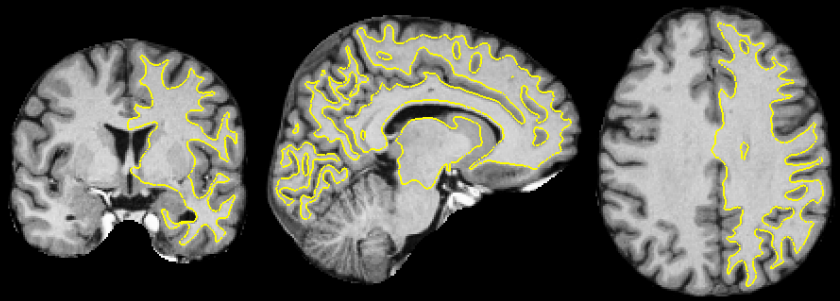

Gray-white boundary

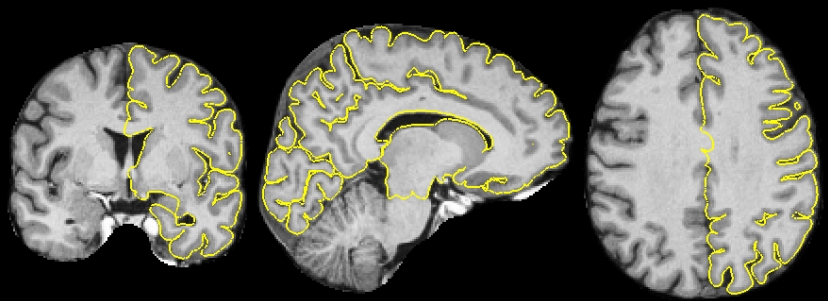

Pial surface

Surface Flattening – Whole Hemisphere

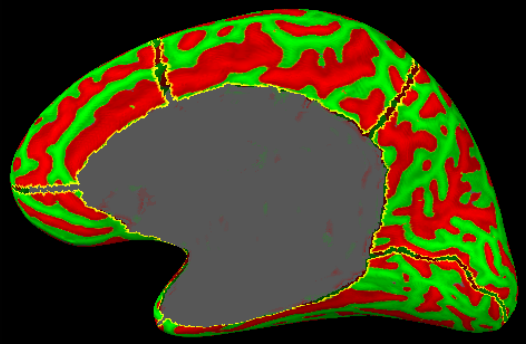

Inflated surface with cuts

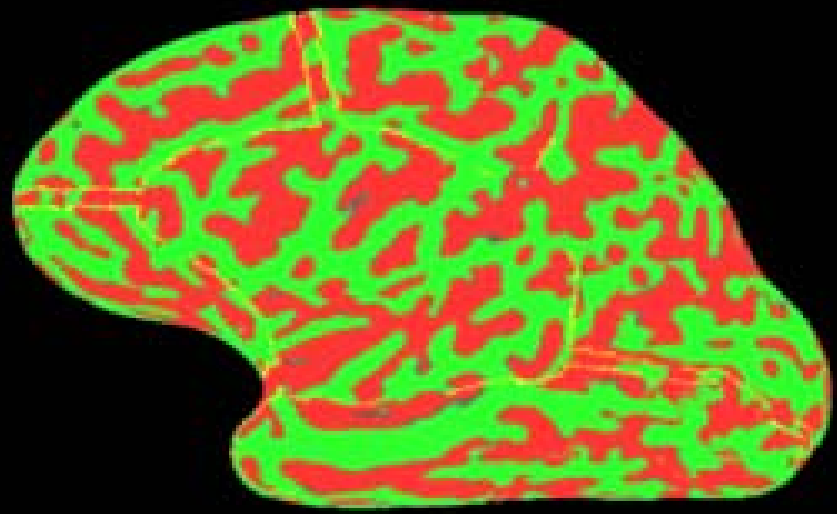

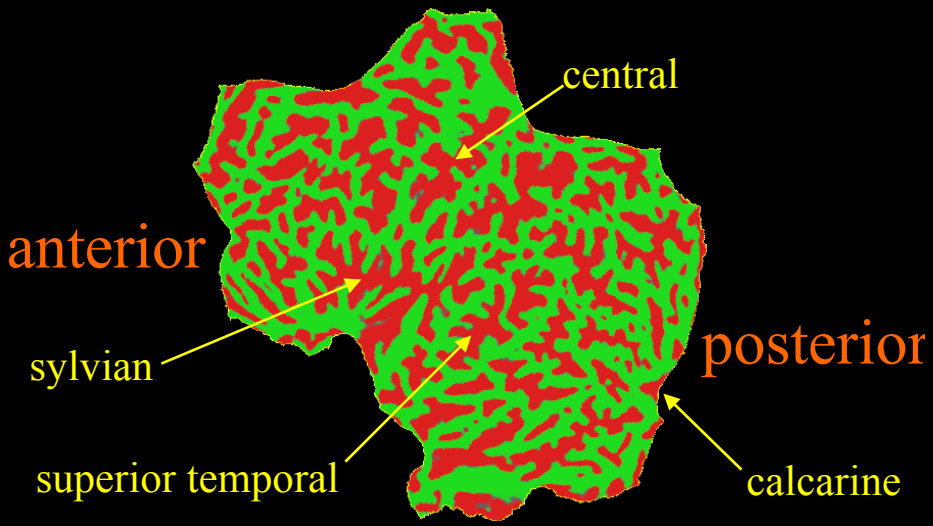

Metrically optimal flat map

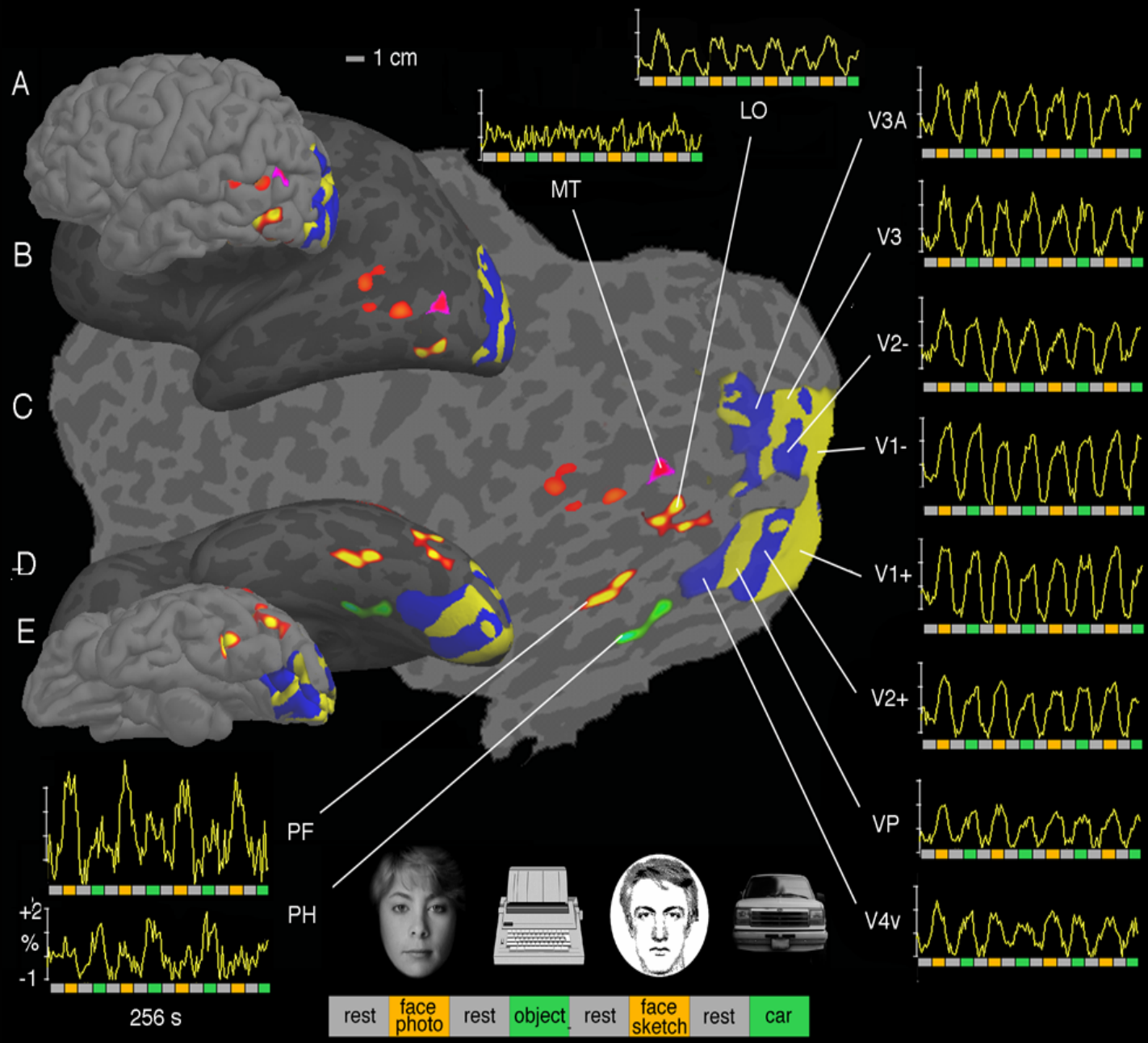

Borrowed from (Halgren et al., 1999)

Talairach Coordinates

Can mean many things, but most common is linear transform to align input image with a target image that is average of many individuals aligned with the atlas of Talairach and Tournoux (1988).

Not Good For Cortex!

1. Typical transform is too low dimensional to account for variability in cortical folds.
2. Landmarks are subcortical (and far from much of cortex).
3. Implicit assumption that 3D metric is appropriate one.

Talairach averaging

Average of 40

Single subject

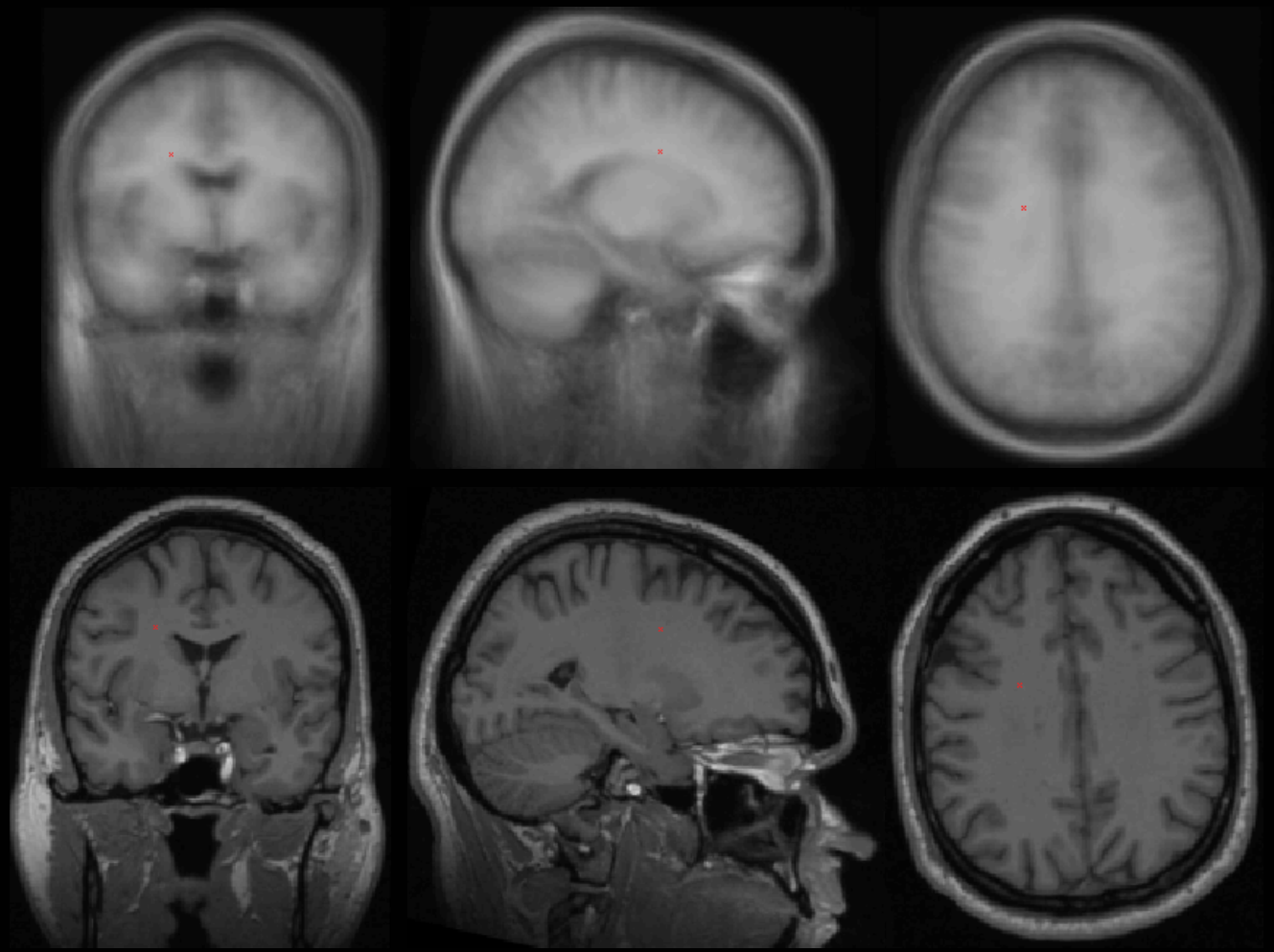

How to align different cortical surfaces?

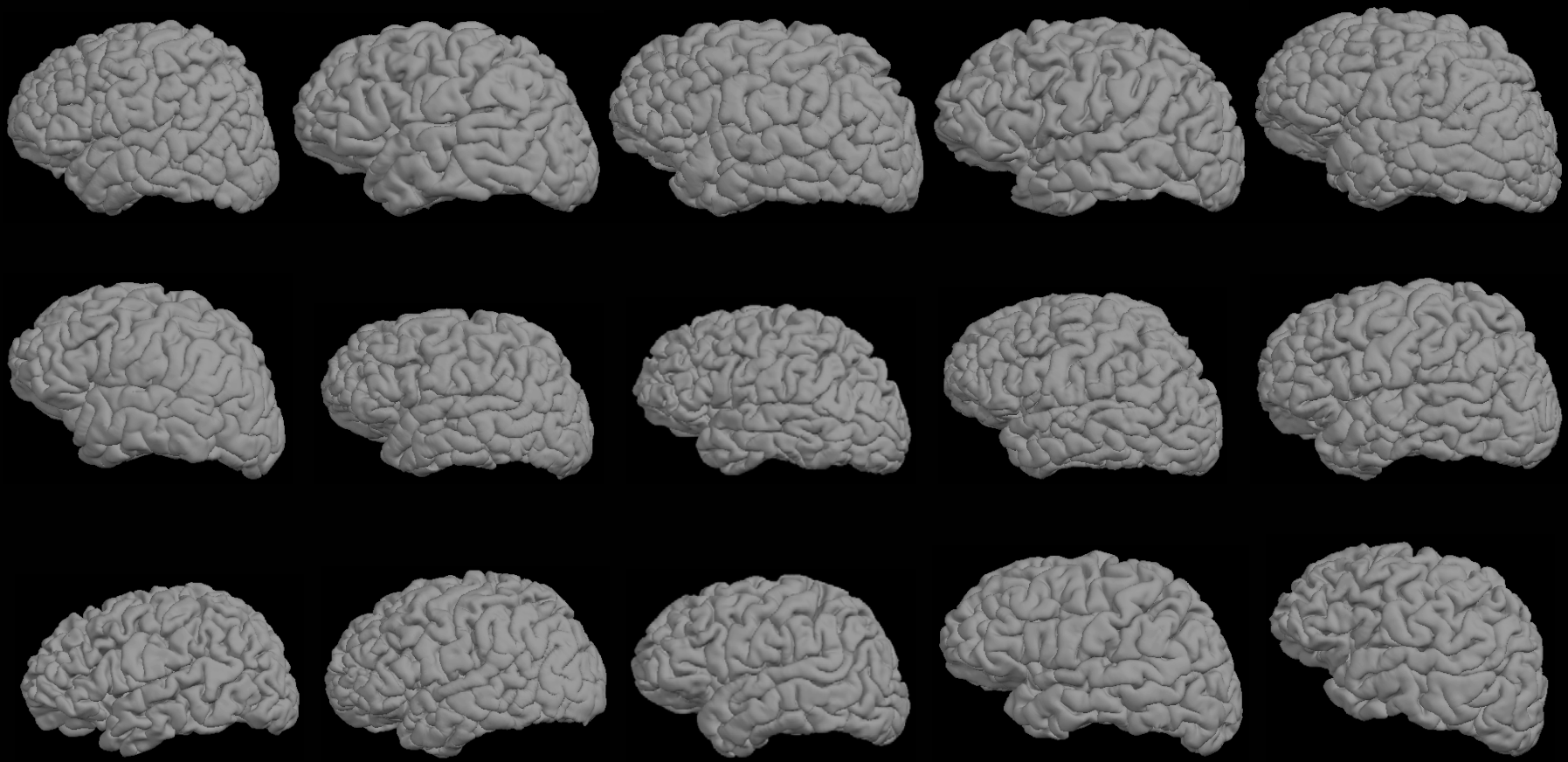

Surface-Based Coordinate System

- Establish a 2-D coordinate system on cortical surface
  - Every point in cortex should have a (unique) coordinate
  - Every coordinate should refer to a point in cortex
- Inter-subject alignment of cortical folding patterns
- Improve alignment of *functional* areas

A Surface-Based Coordinate System

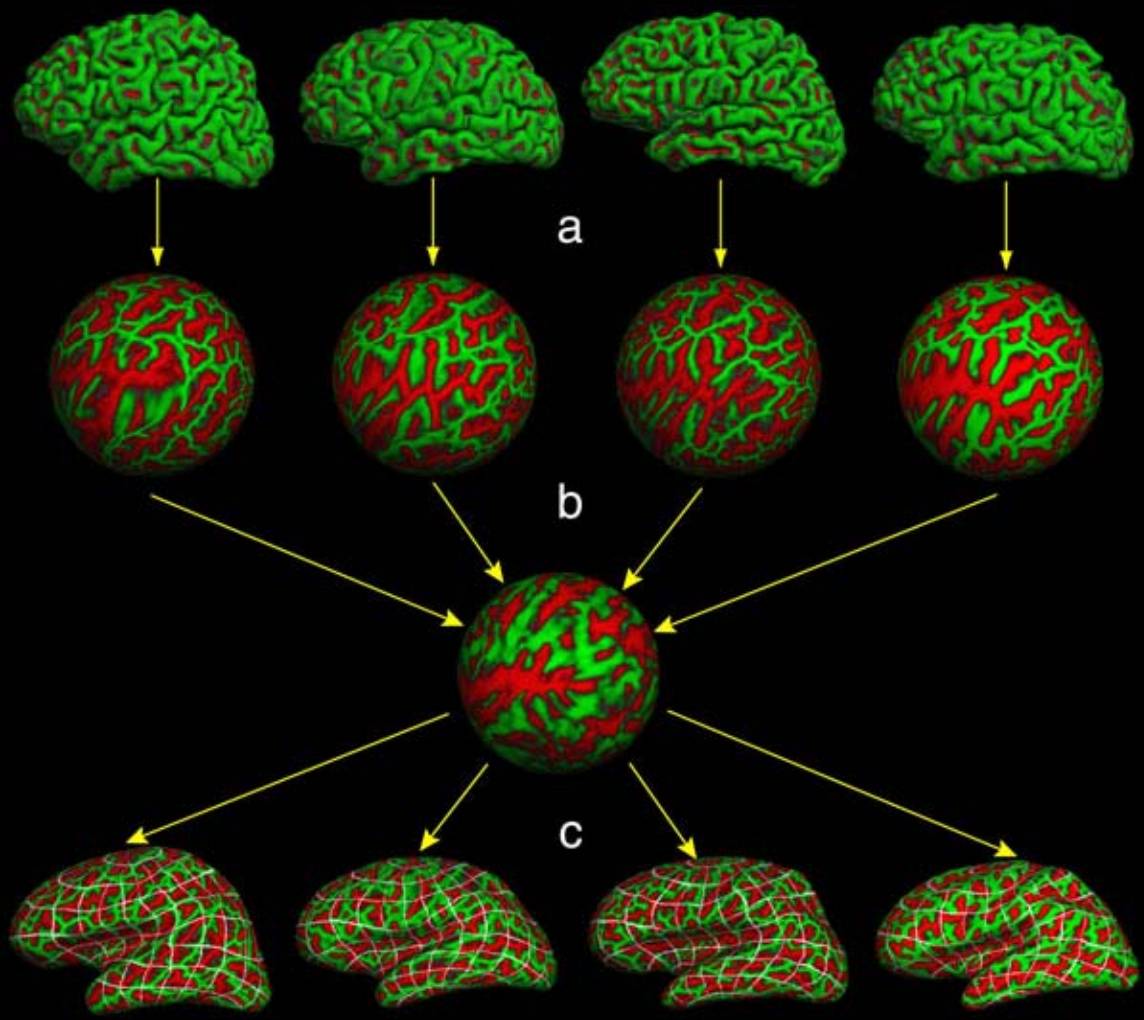

Maximally Isometric Spherical Mapping

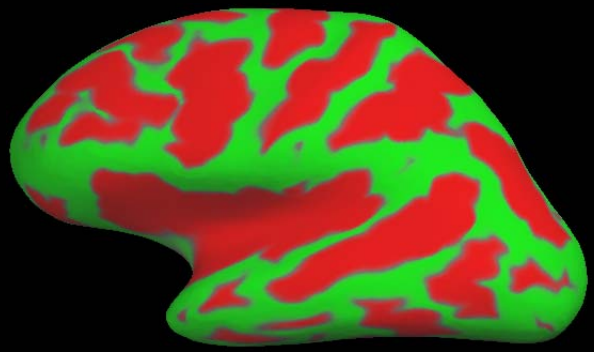

Inflated Surface

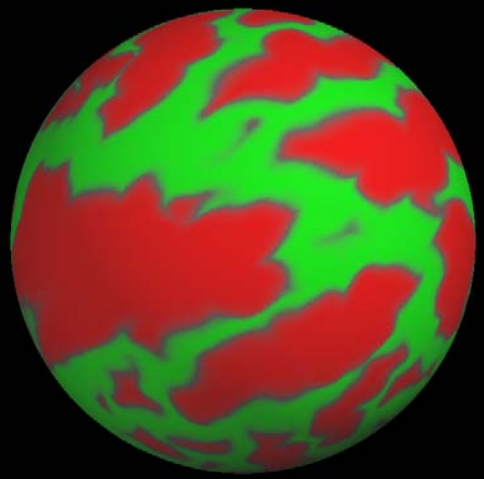

Transformed Surface

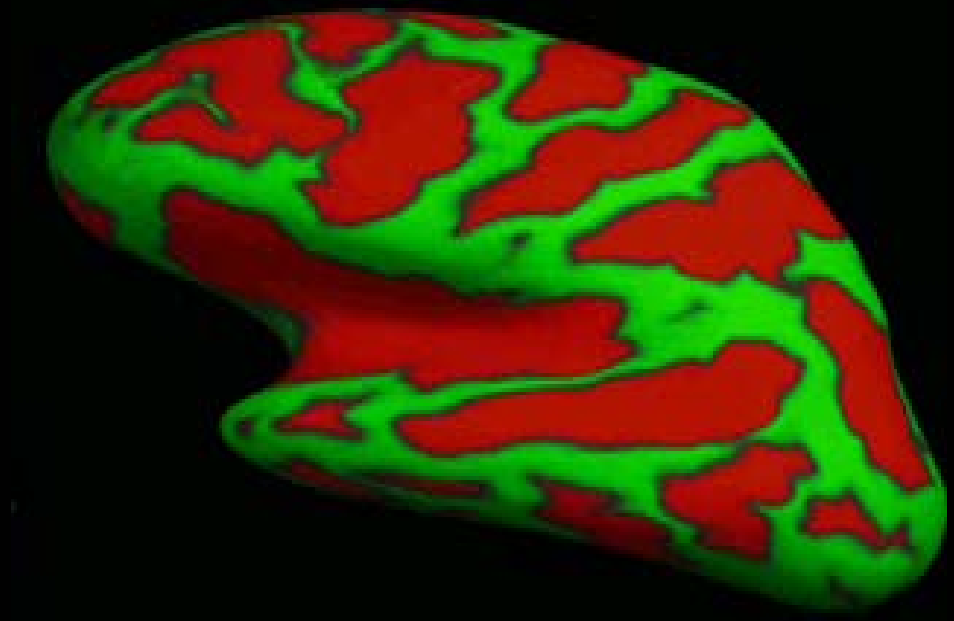

Spherical Morphing: Equations

Energy Functional: $J_c+\lambda_d J_d+\lambda_T J_T$

J_c: Correlation error (aligns folding patterns)

J_d: Metric distortion (constrains allowable shape differences)

J_T: Topology term (forces mapping to be invertible)

Spherical Morphing: Equations

Average Folding Pattern:

$$\overline{C}(\varphi,\theta) = \frac{1}{N}\sum_{i=1}^{N} C_i(\varphi,\theta)$$

Variance of Folding

$$\sigma^2(\varphi,\theta) = \frac{1}{N-1}\sum_{i=1}^{N}(C_i(\varphi,\theta) - \overline{C}(\varphi,\theta))^2$$

Maximum Likelihood Term:

$$J_c = \frac{1}{2V}\sum_{v=1}^{V}\left(\frac{G_\alpha * (C_v - \overline{C}(\phi(v),\theta(v)))}{\sigma(\phi(v),\theta(v))}\right)^2$$

Complete Energy Functional:

$$J = J_c + \lambda_T J_T + \lambda_d J_d$$

Inter-Subject Morphing

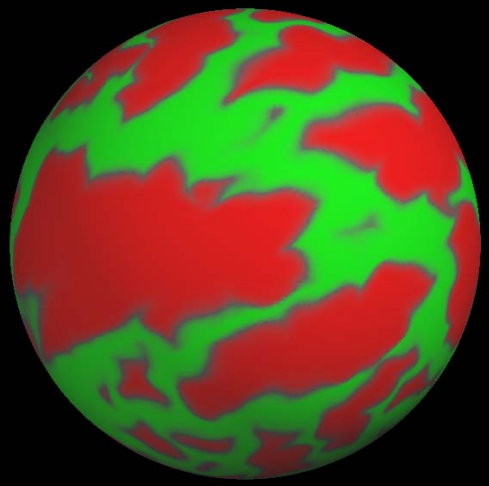

Individual Subject

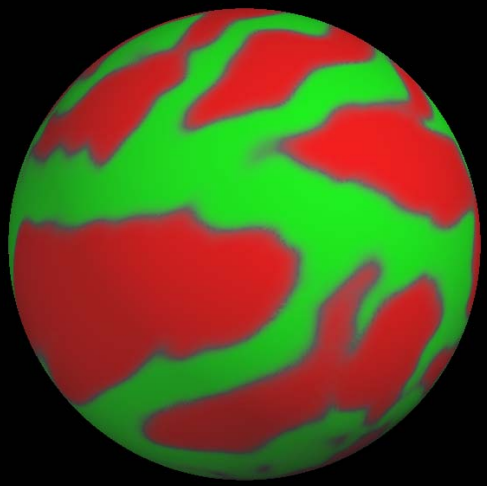

Average (Target)

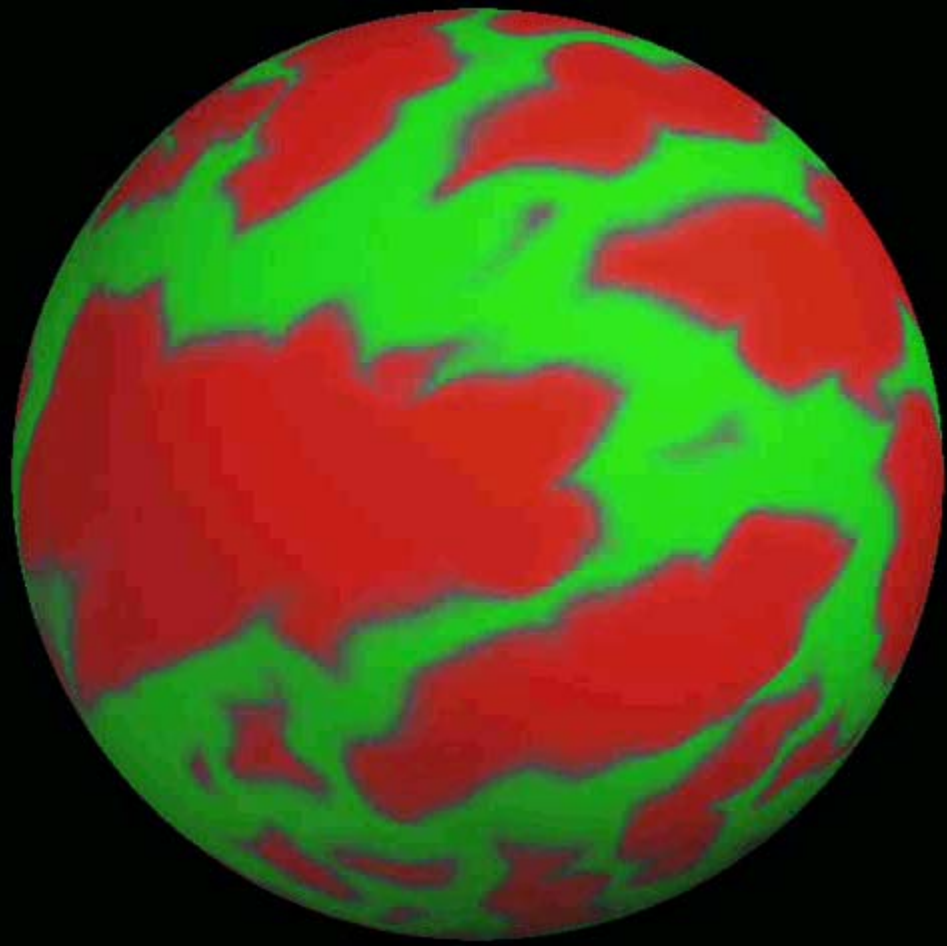

Surface-Based Averaging

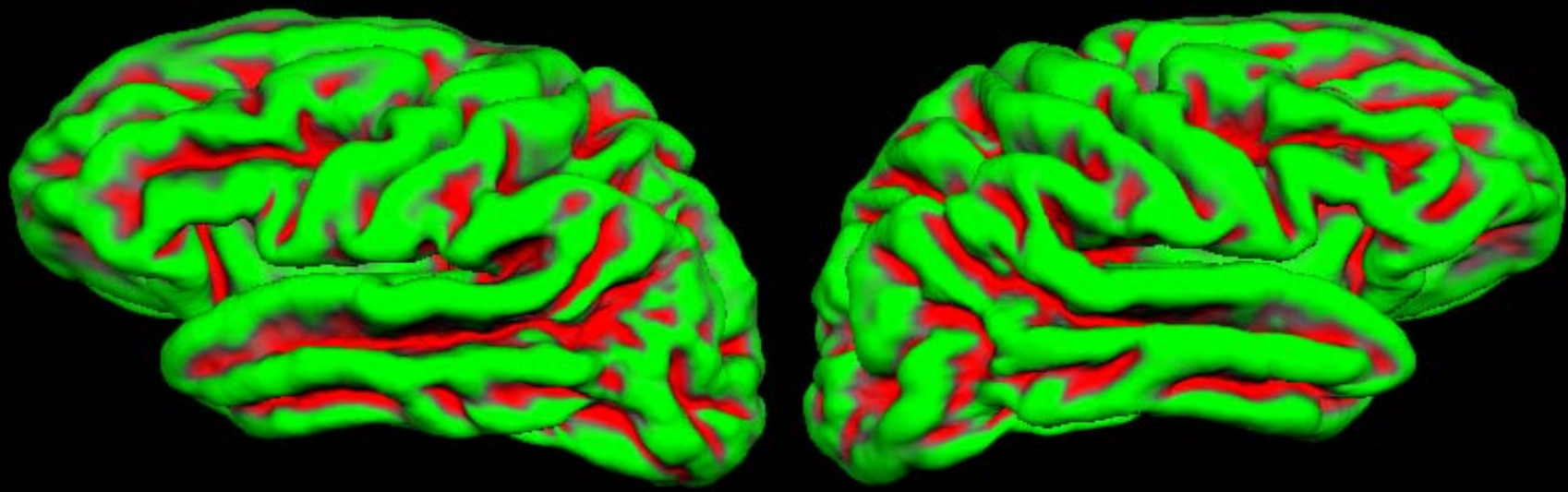

Average surface created from 30 subjects

Applications

- Increased statistical power for inter-subject averaging
- Automatic functional/anatomical labeling
- Inter-subject averaging of morphometric properties
- Statistical analysis of morphometric properties
  - aging
  - neurodegenerative diseases
  - longitudinal studies of structural changes
  - hemispheric asymmetry

Applications

- Increased statistical power for inter-subject averaging
- Automatic functional/anatomical labeling
- Inter-subject averaging of morphometric properties
- Statistical analysis of morphometric properties
  - aging
  - neurodegenerative diseases
  - longitudinal studies of structural changes
  - hemispheric asymmetry

Inter-Subject Averaging of Activations

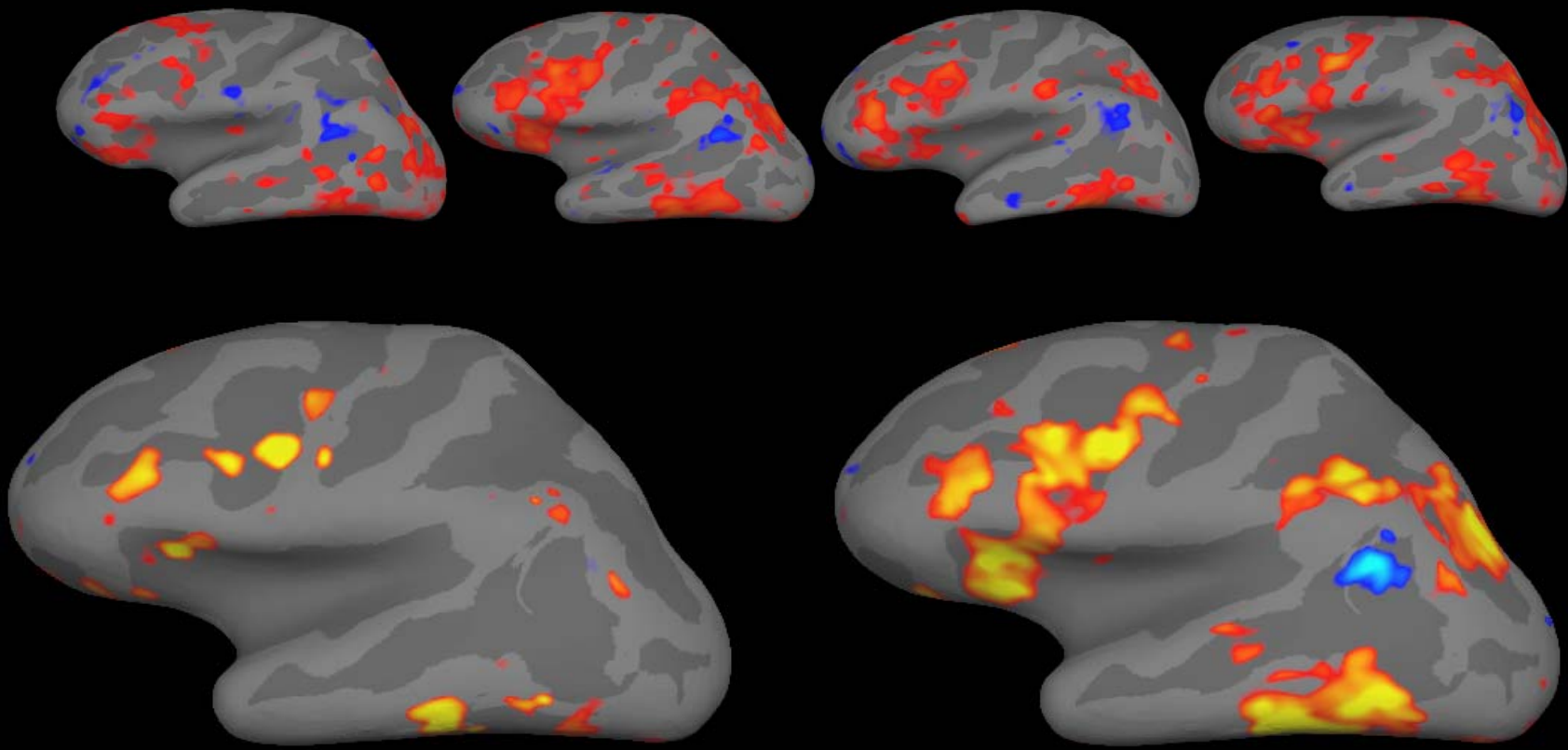

Talairach Average

Spherical Average

Applications

- Increased statistical power for inter-subject averaging
- Automatic functional/anatomical labeling
- Inter-subject averaging of morphometric properties
- Statistical analysis of morphometric properties
  - aging
  - neurodegenerative diseases
  - longitudinal studies of structural changes
  - hemispheric asymmetry

Applications

- Increased statistical power for inter-subject averaging
- Automatic functional/anatomical labeling
- Inter-subject averaging of morphometric properties
- Statistical analysis of morphometric properties
  - aging
  - neurodegenerative diseases
  - longitudinal studies of structural changes
  - hemispheric asymmetry

Cortical Parcellation: Manual vs. Automated

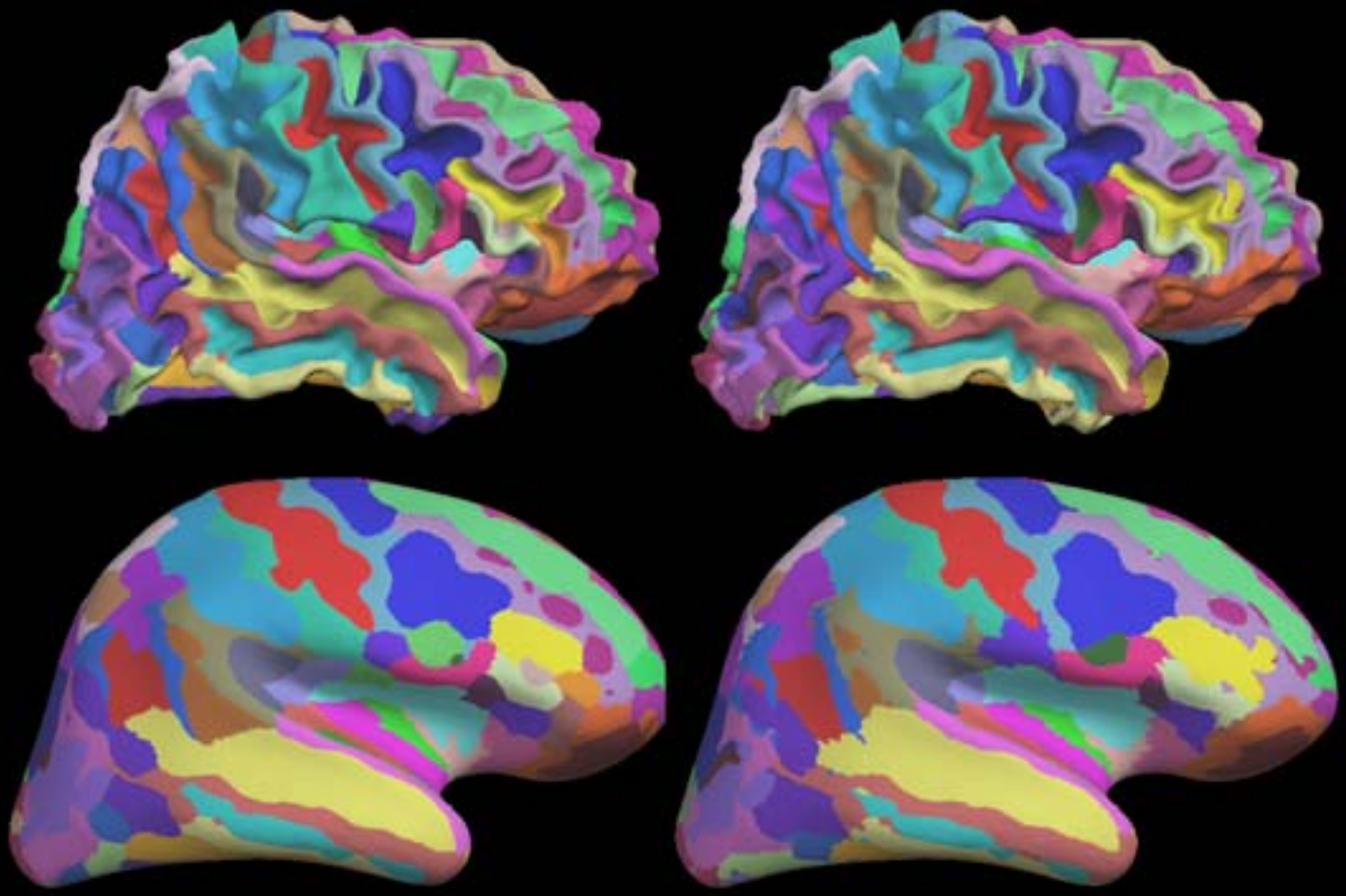

Manual Parcellation Automatic Parcellation

Thanks to Christophe Destrieux for this slide.

Applications

- Increased statistical power for inter-subject averaging
- Automatic functional/anatomical labeling
- Inter-subject averaging of morphometric properties
- Statistical analysis of morphometric properties
  - aging
  - neurodegenerative diseases
  - longitudinal studies of structural changes
  - hemispheric asymmetry

Applications

- Increased statistical power for inter-subject averaging
- Automatic functional/anatomical labeling
- Inter-subject averaging of morphometric properties
- Statistical analysis of morphometric properties
  - aging
  - neurodegenerative diseases
  - longitudinal studies of structural changes
  - hemispheric asymmetry

Selective Regional Thinning in AD

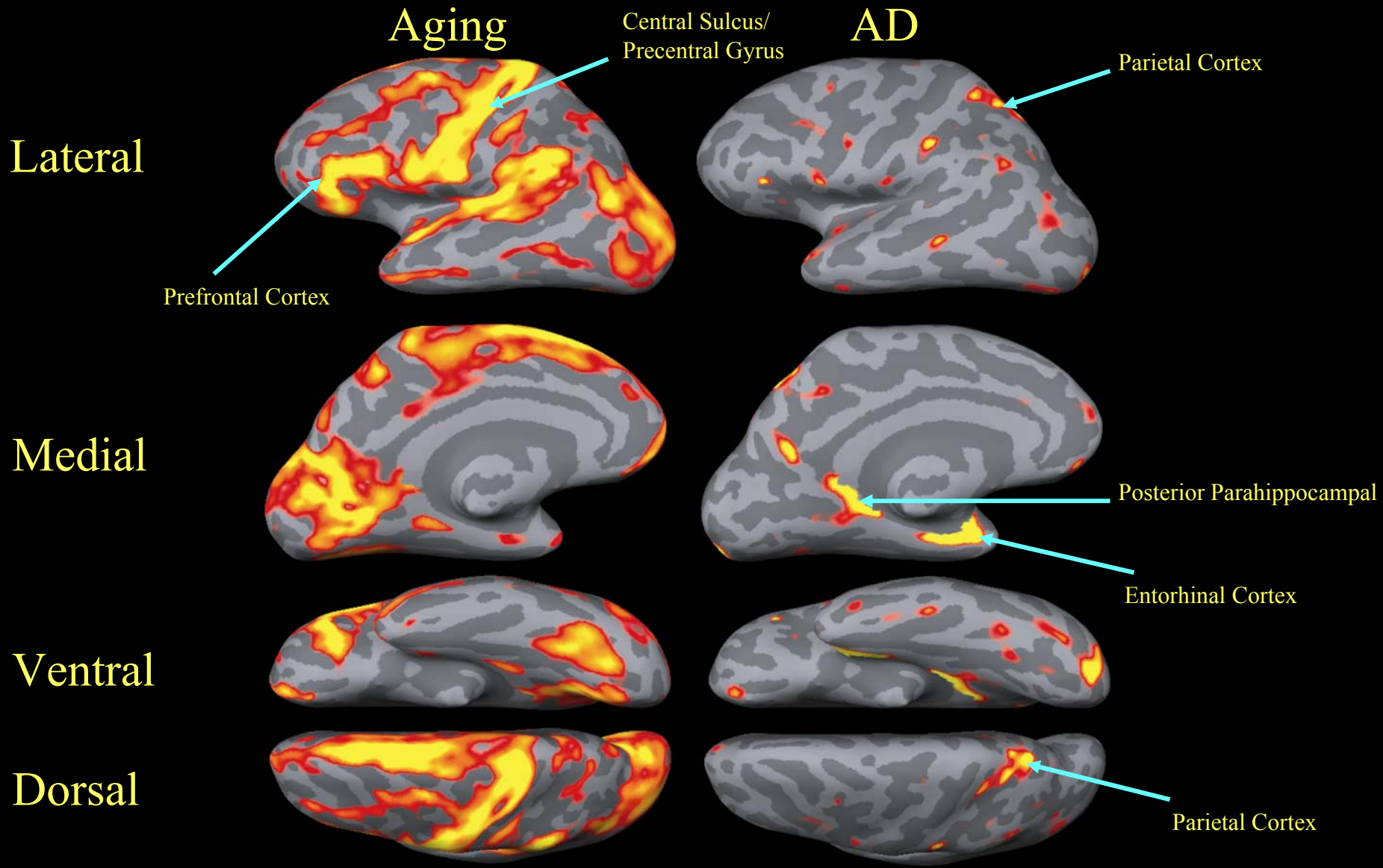

Courtesy of Drs. Randy Buckner and David Salat

Talk Outline

1. Cortical Analysis.
2. Subcortical Analysis.
3. Sources of distortion in MRI.
4. Linking micro structure to macro structure.

Talk Outline

1. Cortical Analysis.
2. Subcortical Analysis.
3. Sources of distortion in MRI.
4. Linking micro structure to macro structure.

Whole-Brain Segmentation

Goal: Segment T1-weighted MRI into anatomically and semantically meaningful structures (e.g. caudate, putamen, etc…).

Requirements:

- Insensitive to pathology.
- Insensitive to varying pulse sequences.

Prerequisite: registration with anatomically meaningful space (e.g. Talairach)

Why Segmentation is Hard!

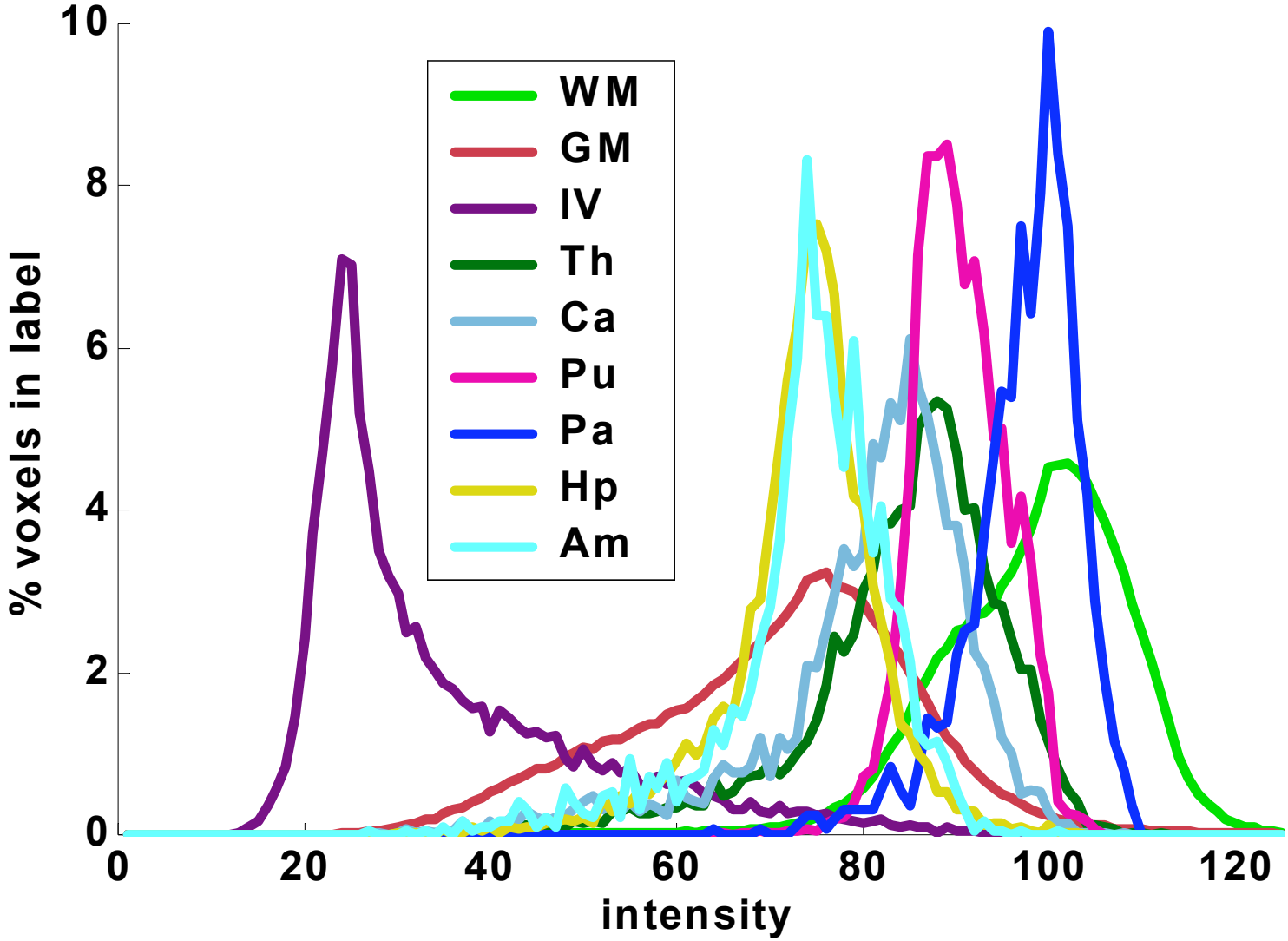

Inter-subject Registration

Goal: align functionally homologous points across subjects (e.g. hippocampus with hippocampus, amygdala with amygdala, etc…).

Problem: this information is in general unavailable

Typical solution: align image intensities and hope this results in alignment of function/structure as well.

What does Mean-Squared Error Estimation mean from a Probabilistic Perspective?

Find *f* that minimizes $\iiint (I(f(\mathbf{r})) - T(\mathbf{r}))^2 d\mathbf{r}$

(*T* is target image, *I* is input image, *r* is spatial coordinate)

Assume $\log(p(I \mid f, T)) = \iiint -(I(f(\mathbf{r})) - T(\mathbf{r}))^2 d\mathbf{r}$

Then: $p(I \mid f, T) = \prod e^{-(I(f(\mathbf{r})) - T(\mathbf{r}))^2}$

→ *f* is the maximum likelihood solution assuming the image noise can be modeled as a set of IID random variables with means *T(r)* and equal (unit) variances.

Mean-squared Error Registration: Low Quality Data

I(r)

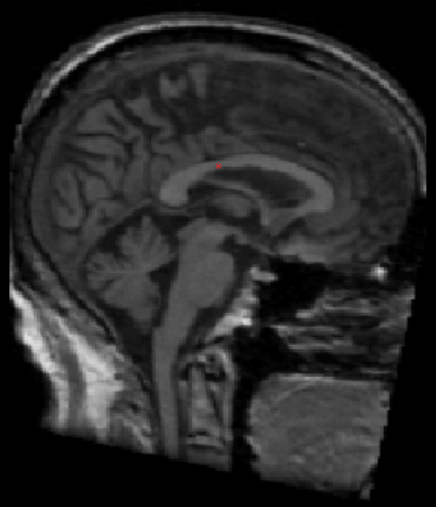

T(r)

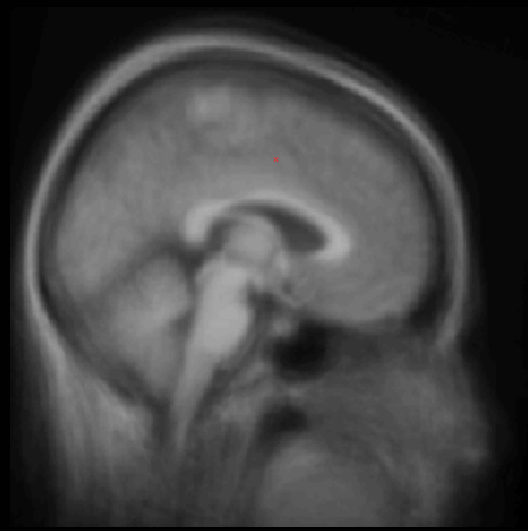

I(Lr)

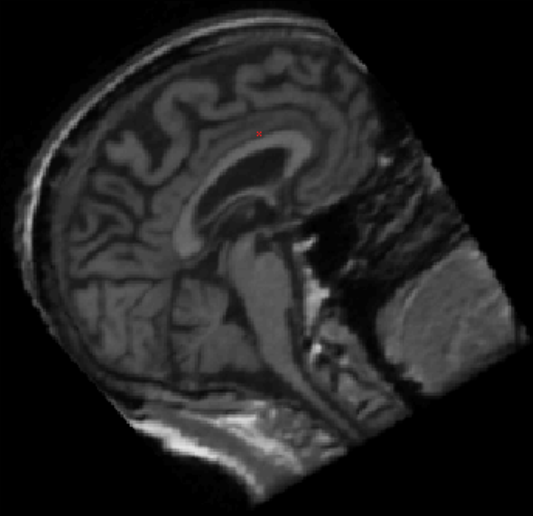

Mean-squared Error Registration

Anatomy is variable, particularly in cases of pathology*

→ *A given spatial location may contain a different tissue class in different types of subjects!*

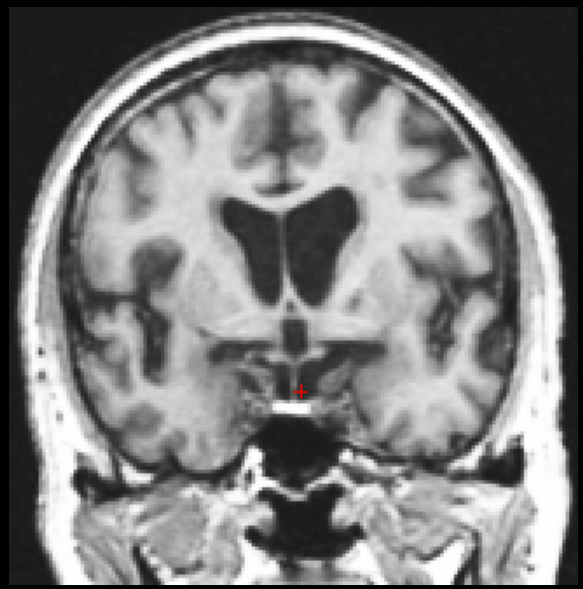

* Thanks to Marilyn Albert and Ron Killiany for providing this data.

Segmentation-based Registration

Find the transformation that maximizes the probability that each point in the individual is drawn from *one* of the tissue classes in the template.

Find the *L* that maximizes the probability of observing image *I* given the segmentation *C*:

$$L = \arg\max p(I \mid L, C)$$

How do we find the segmentation C?

Segmentation-based Registration

Problem of finding *L* is highly overdetermined (many, many more data points than parameters to solve for).

Can assume *C* in certain atlas locations (a few thousand) where prior probabilities are high, and use them to find *L* using a *global* search (local minima/maxima not a problem).

Atlas Points After Registration

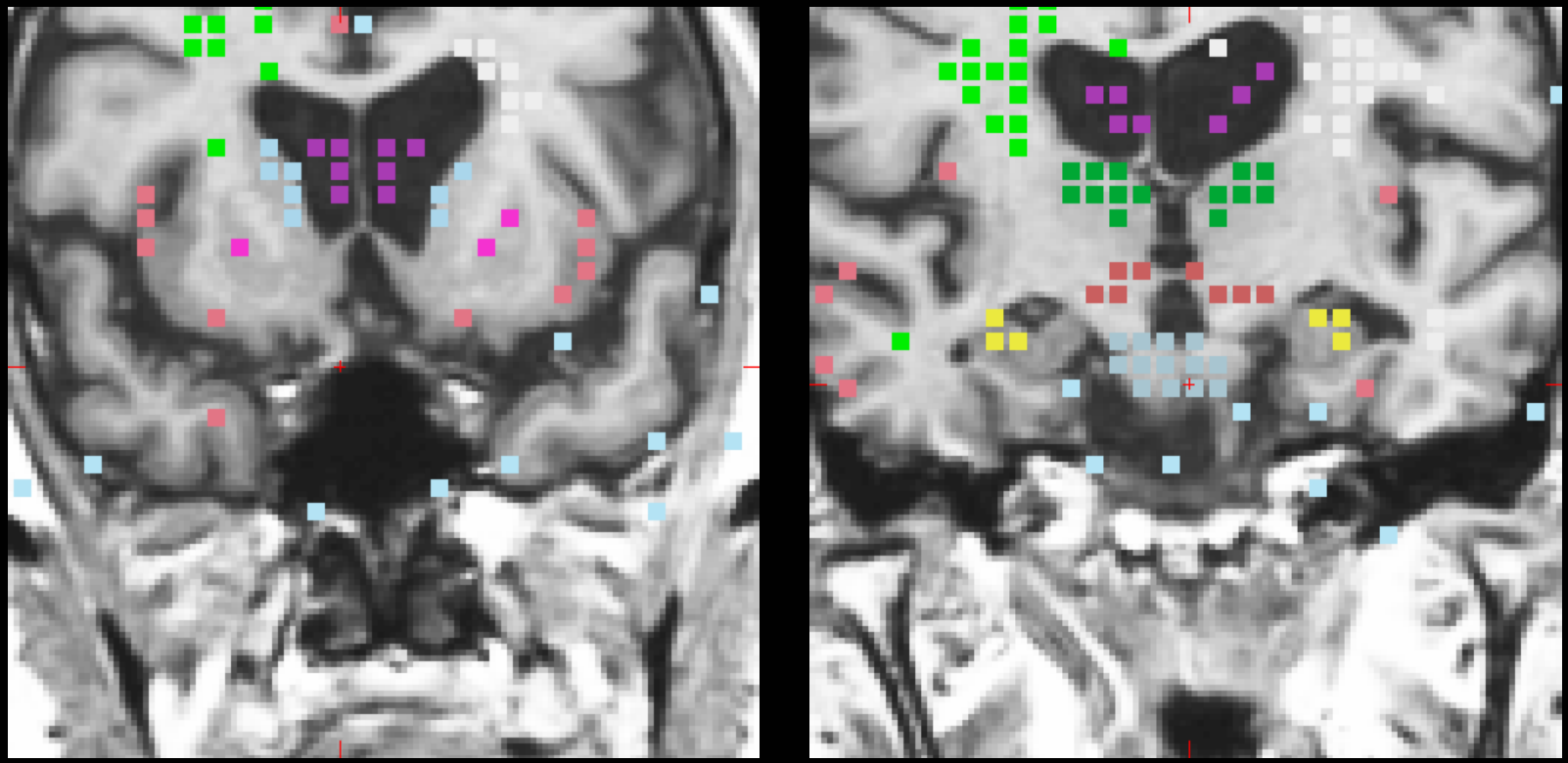

Segmentation-based Registration: Results

Normal

AD

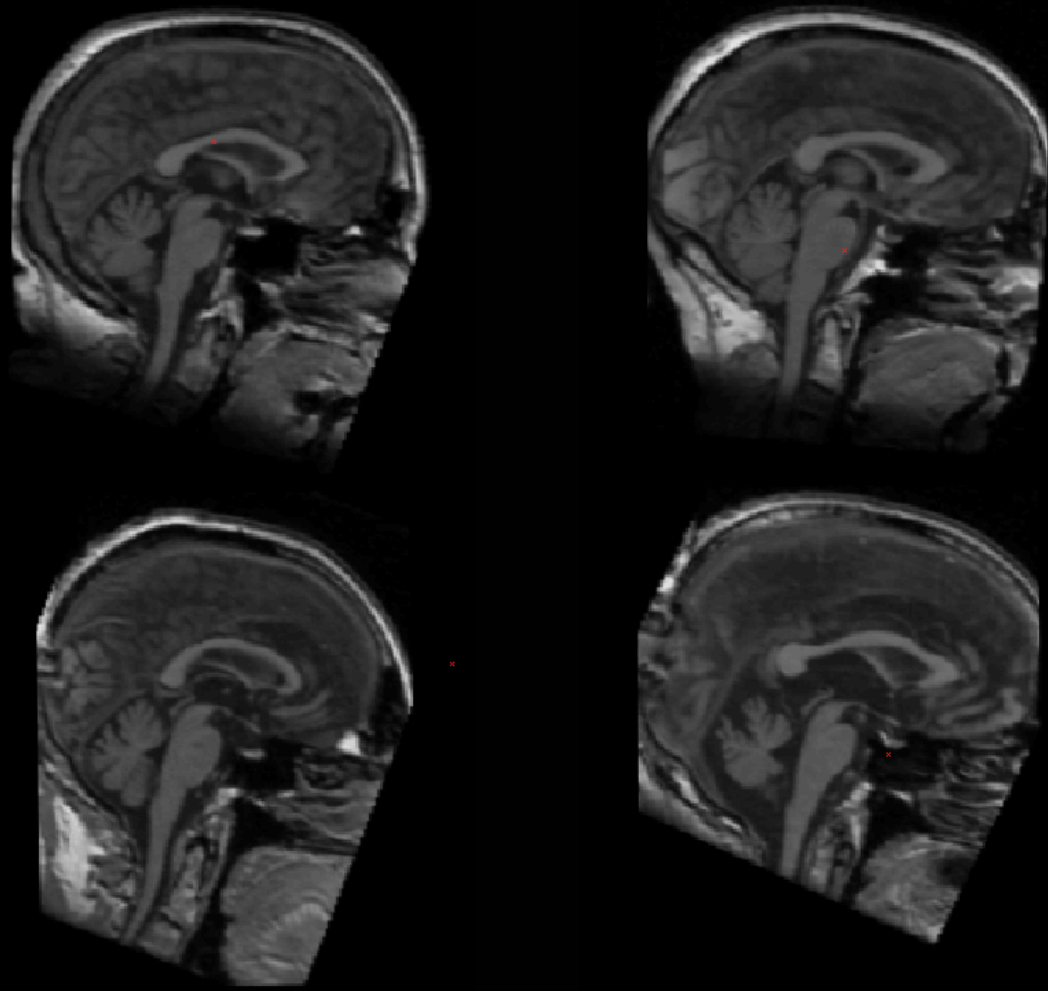

Segmentation Results: CMA Labeling

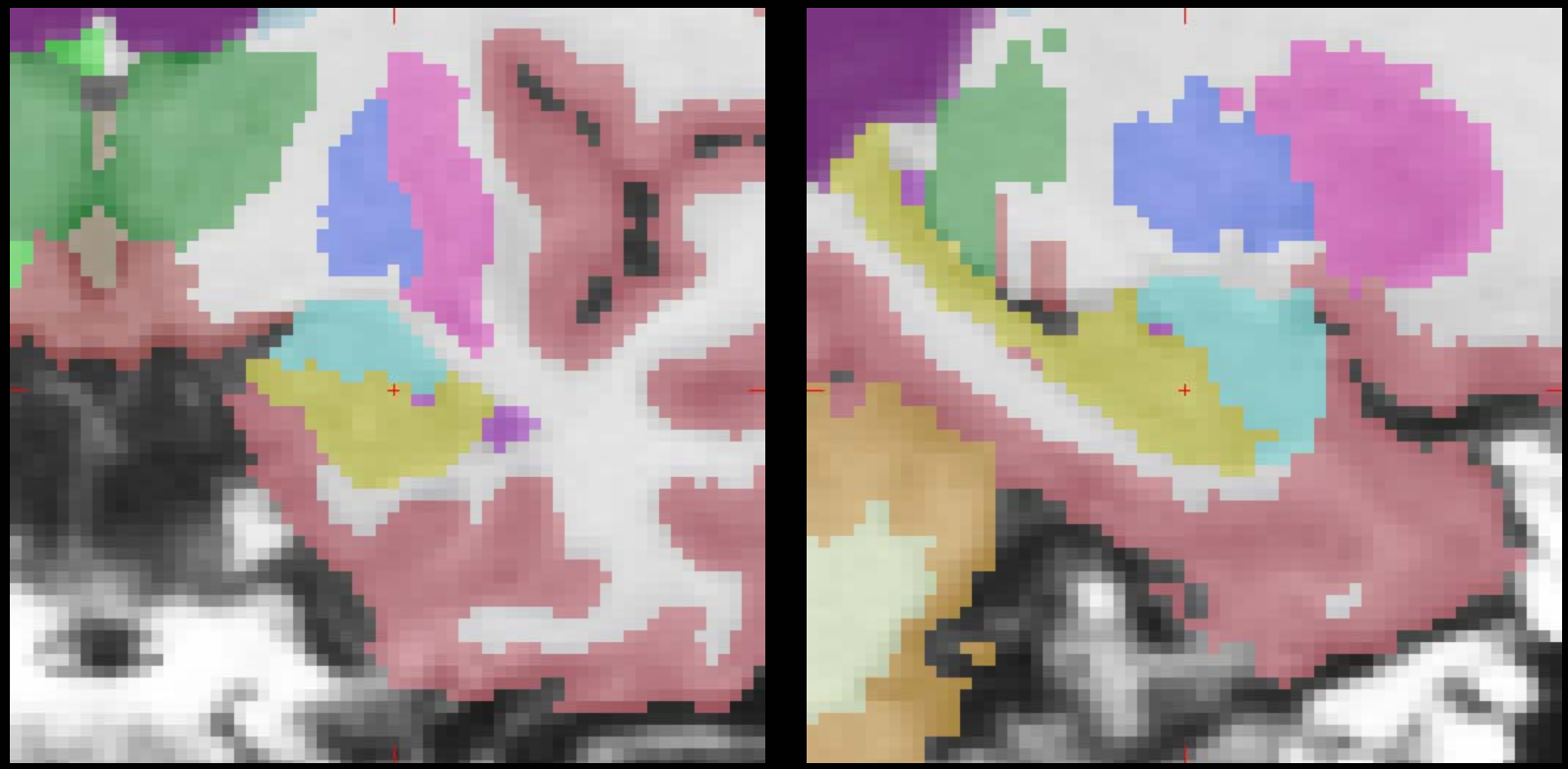

- Cerebellar cortex
- Cerebellar WM
- 4th ventricle
- RH cerebral WM
- LH cerebral WM
- Hippocampus
- LH pallidum
- Thalamus
- Cerebral cortex
- Misc.
- Lateral ventricle
- Caudate
- Amygdala

Tissue Segmentation

Given a transform *f* into an atlas space, *C* can be estimated using a Maximum a Posteriori (MAP) approach: what is the most likely tissue classification *C* given the observed image *I* , the transformation *f*, and prior information about *C*?

$$C = \arg\max_{C'} p(C' \mid I, f)$$

$$p(C' \mid I, f) \sim p(I \mid C', f)\, p(C')$$

What prior information *p(C)* can we use to constrain the allowable segmentations?

Tissue Segmentation

The probability distribution of each voxel is modeled as an independent *nonstationary* Gaussian (because it is a function of ***r***):

$$p(I \mid f, C) = \prod_{\mathbf{r} \in R} p(I(\mathbf{r}) \mid f, C(\mathbf{r}), \mathbf{r})$$

Forward Model of Image Formation:

$$p(I(\mathbf{r}) \mid f, C(\mathbf{r}) = c, \mathbf{r}) = \frac{1}{\sigma_c(f(\mathbf{r}))\sqrt{2\pi}} \exp\left(-\frac{(I(\mathbf{r}) - \mu_c(f(\mathbf{r})))^2}{\sigma_c(f(\mathbf{r}))^2}\right)$$

Note: can make $\mu_c(f(\mathbf{r}))$ a function of MR parameters and embed physics of imaging into forward model (more later)

Gibbs Priors: Motivation

What is the probability that cortical gray matter occurs inferior to hippocampus?

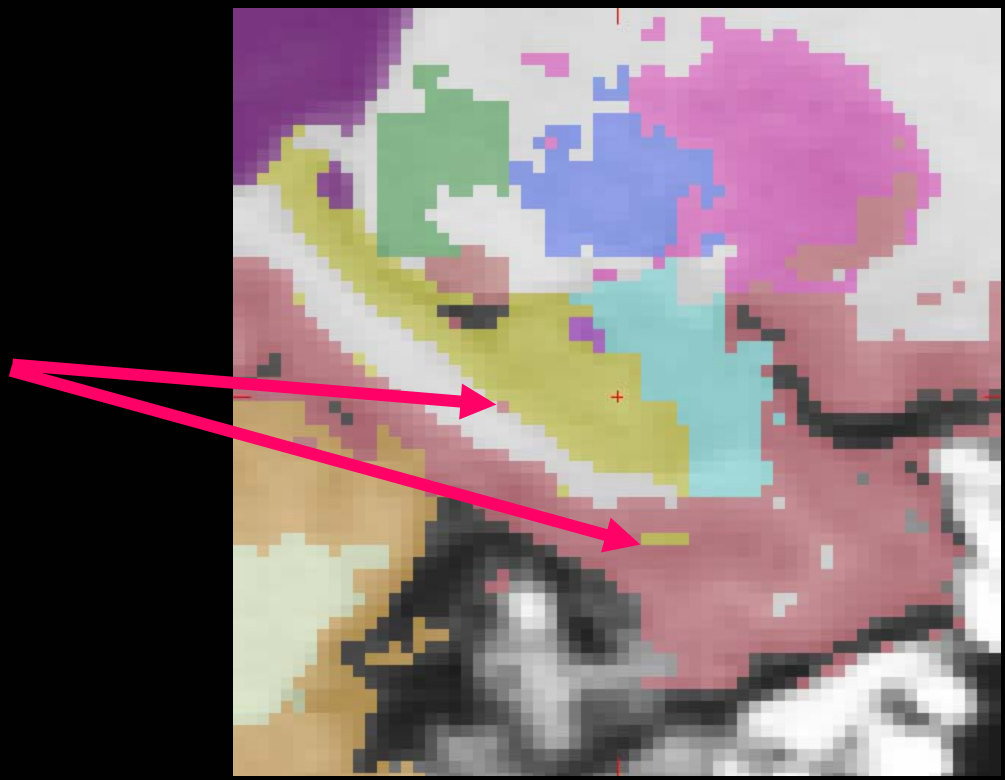

Markov Random Fields

Modeling the segmentation as a *Markov Random Field (MRF)* means:

$p(C(\mathbf{r})|\text{the rest of the labels}) = p(C(\mathbf{r})|\text{labels in a neighborhood around } \mathbf{r})$

Segmentation: MRF

Problem: the segmentation is fractured because no spatial smoothness constraints are encoded in model.

Solution: incorporate prior probability of one tissue class being the neighbor of another into model:

$$p(C) \propto \prod_{\mathbf{r} \in R} p(C(\mathbf{r}) \mid \mathbf{r}) \prod_{\mathbf{r}_i \in N(\mathbf{r})} p(C(\mathbf{r}_i) \mid C(\mathbf{r}), i, \mathbf{r}, \mathbf{r}_i)$$

Segmentation: MRF

$p(\mathrm{C}(\boldsymbol{r}_i)|C(\boldsymbol{r}), I, \boldsymbol{r},\boldsymbol{r}_i)$ encodes the probability that tissue class $\mathrm{C}(\boldsymbol{r}_i)$ occurs at spatial location r_i when tissue class $C(\boldsymbol{r})$ occurred at $\boldsymbol{r}$. The segmentation is thus modeled as an *anisotropic* nonstationary *MRF*.

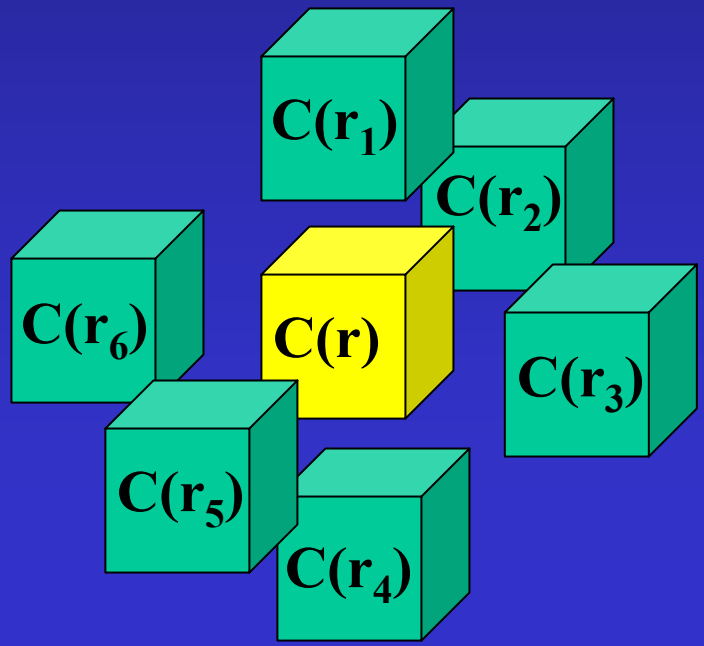

Segmentation: MRF

Preliminary Segmentation

Final Segmentation

Segmentation with MRF: Fly Through

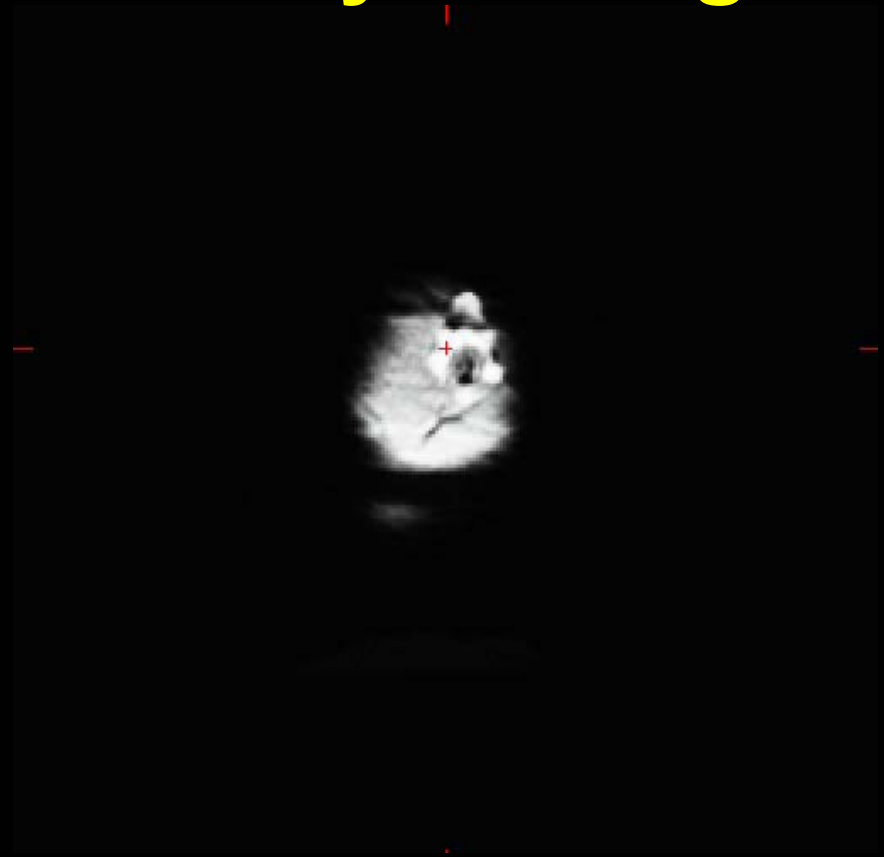

Cerebellar cortex
Cerebellar WM
4th ventricle
RH cerebral WM
LH cerebral WM
Hippocampus
LH pallidum
Thalamus
Cerebral cortex
Misc.
Lateral ventricle
Caudate
Amygdala

Volume Differences Predictive of AD

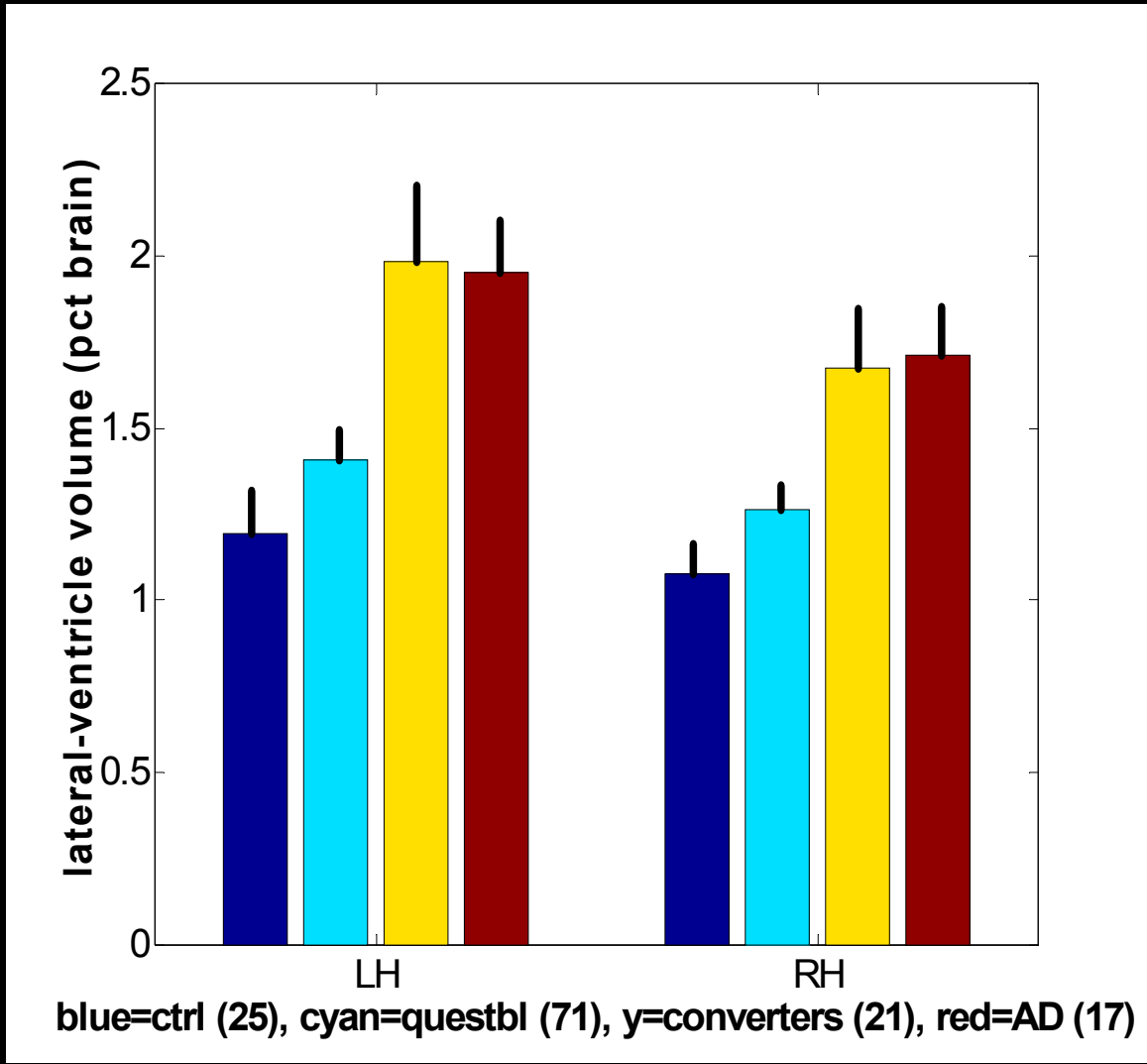

Data courtesy of Drs Marilyn Albert Ron Killiany

Optimizing CNR for Segmentation

Problem: CNR varies over brain because of intrinsic tissue property inhomogeneities, bias fields, etc….

Global CNR dramatically underestimates true CNR. Need a local measure that reflects the true difficulty of the segmentation problem.

Solution: Use atlas to compute local segmentation ambiguity and integrate across brain.

Estimation of Intrinsic Tissue Parameters

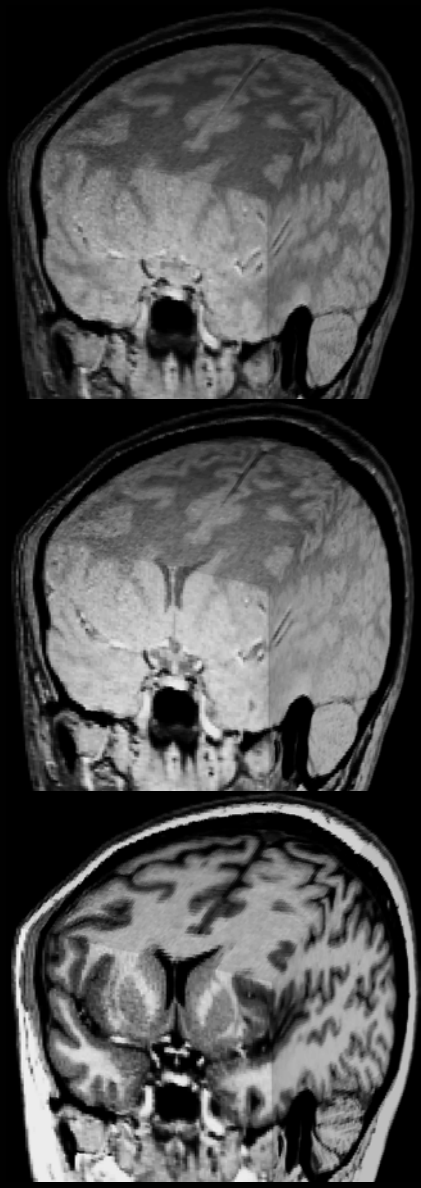

Inverse Bloch Eq.

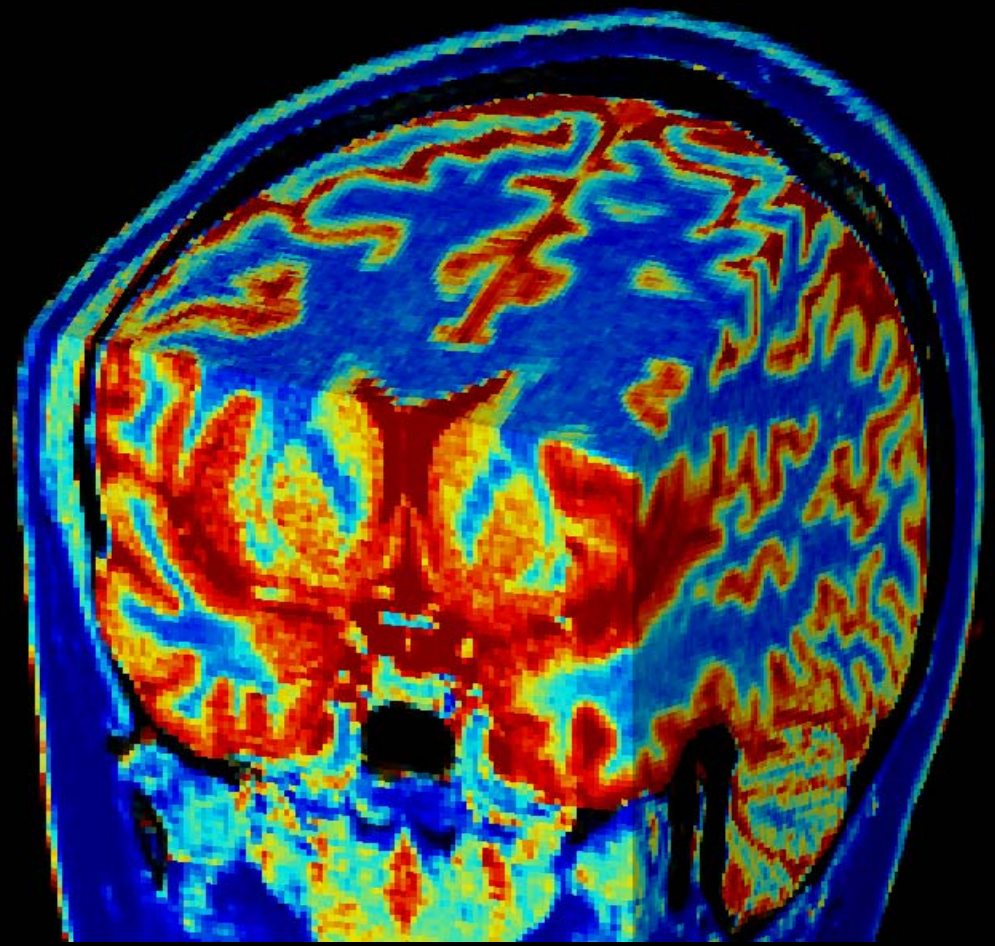

Estimated T_1 values

$$S(TR, TE, \alpha, T_1, T_2^*, P) = \frac{P \sin\left(k(\mathbf{r})\alpha\right)}{k(\mathbf{r})} \left(\frac{1 - e^{-TR/T_1}}{1 - \cos\left(k(\mathbf{r})\alpha\right) e^{-TR/T_1}}\right) e^{-TE/T_2^*}$$

Pulse Sequence Independent Segmentation

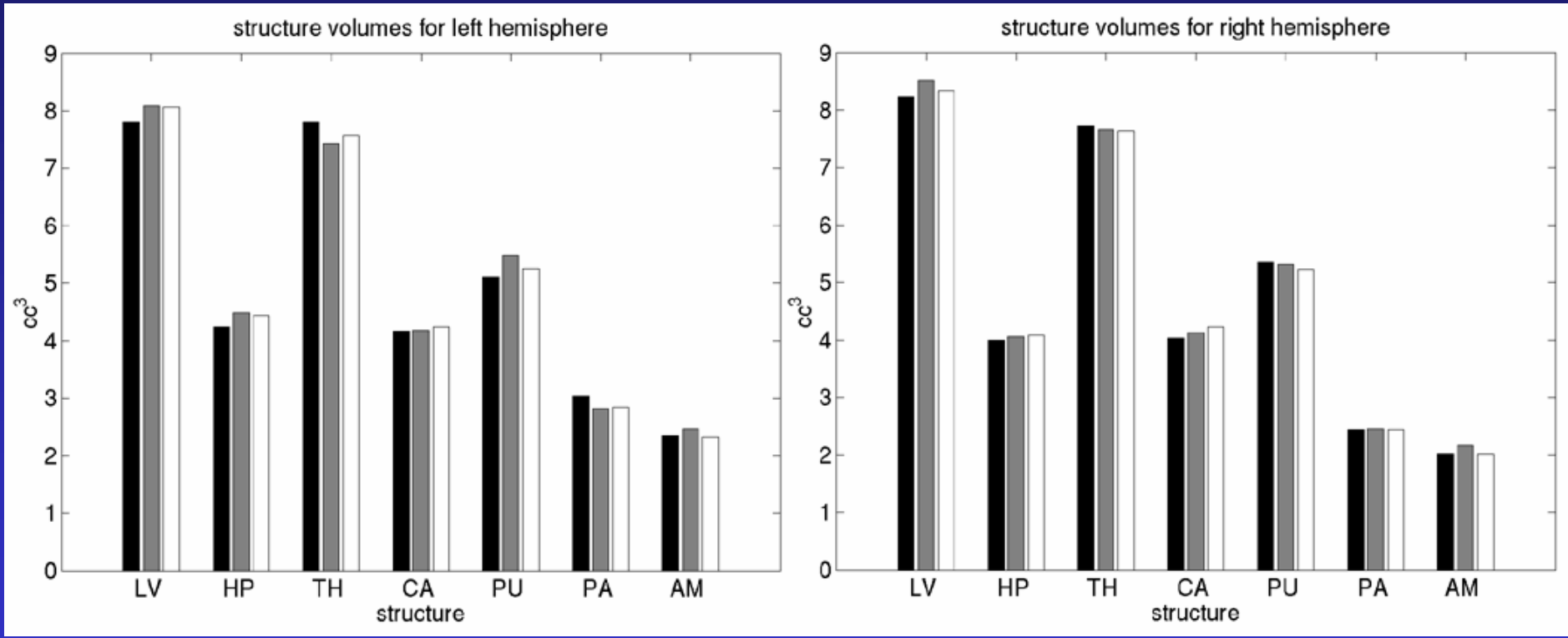

Test-retest structure volumes measured from three separate datasets (dark, medium and light bars) acquired on the same subject. Each dataset had different acquisition parameters (LV=lateral ventricle, HP=hippocampus, TH=thalamus, CA=caudate, PU=putamen, PA=pallidum, AM=amygdala).

Sequence Optimization

$$M = \arg\min A(M) = \iiint_{\mathbf{r}} \sum_{c_2 \neq c_1} \sum_{c_1} \frac{1}{2} \left(p(c_1 \mid c_2, M) + p(c_2 \mid c_1, M) \right)$$

$$p(c_1 \mid c_2, M) = \iint_{\mathbf{I}} p(c_1)\, p(I \mid c_1, M)\, p(I \mid c_2, M)\, d\mathbf{I}$$

$$p(I \mid c_1, M) \sim N(\hat{\mu}_{c_1}(M), \hat{\Sigma}_{c_1}(M))$$

$$\hat{\mu}_c(M) = S(M_{\text{predicted}}, \beta(M_{\text{training}}, \mu_c))$$

$$\hat{\Sigma}_c(M) = J_{\text{predicted}} (J^{+}_{\text{training}} \Sigma_c J^{+T}_{\text{training}}) J^{\text{T}}_{\text{predicted}} + \lambda Id$$

Where J_i is the Jacobian of $S(M_i, \beta)$, and A^+ and A^T are the pseudoinverse and transpose of A respectively.

Predicting Means and Covariances

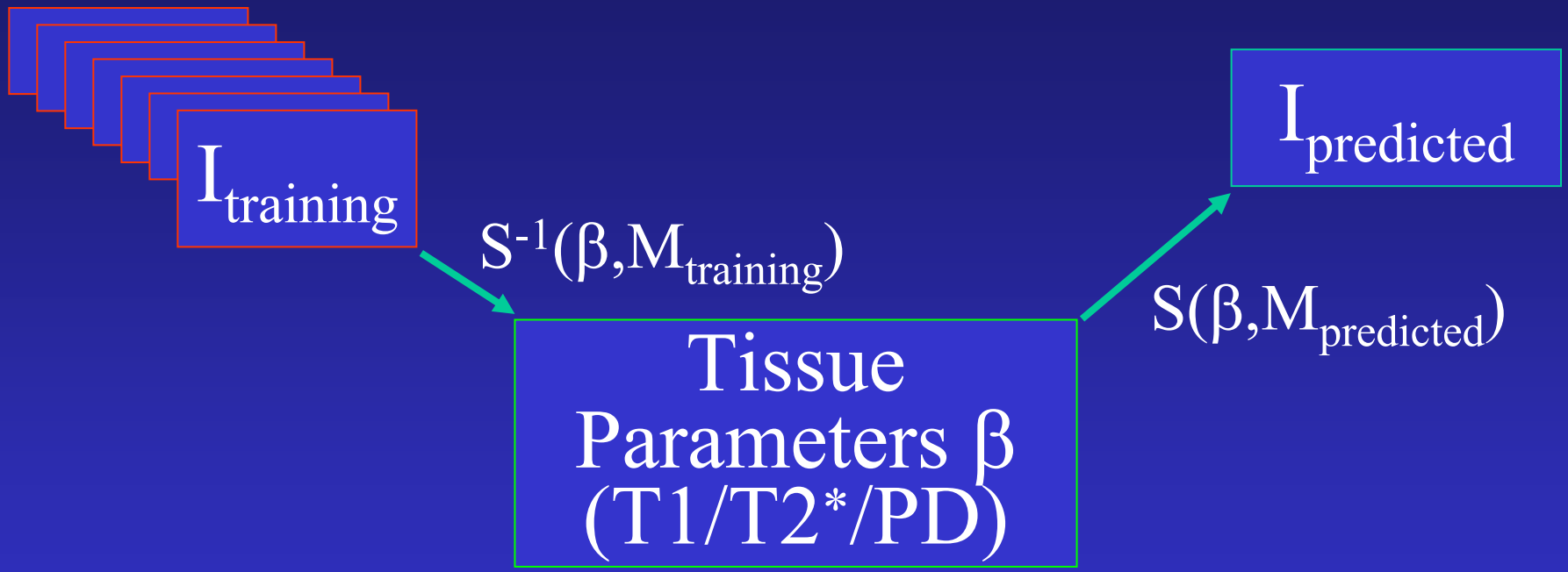

$$\hat{\mu}_c(M) = S(M_{\text{predicted}}, \beta(M_{\text{training}}, \mu_c))$$

$$\hat{\Sigma}_c(M) = J_{\text{predicted}}(J^{+}_{\text{training}} \Sigma_c J^{+T}_{\text{training}}) J^{\text{T}}_{\text{predicted}} + \lambda Id$$

Where M_i are the MR pulse parameters used in acquisition i.

Ambiguity for 2 flip angles

(2 flash scans, TR=20ms, TE=3ms, 18 subjects)

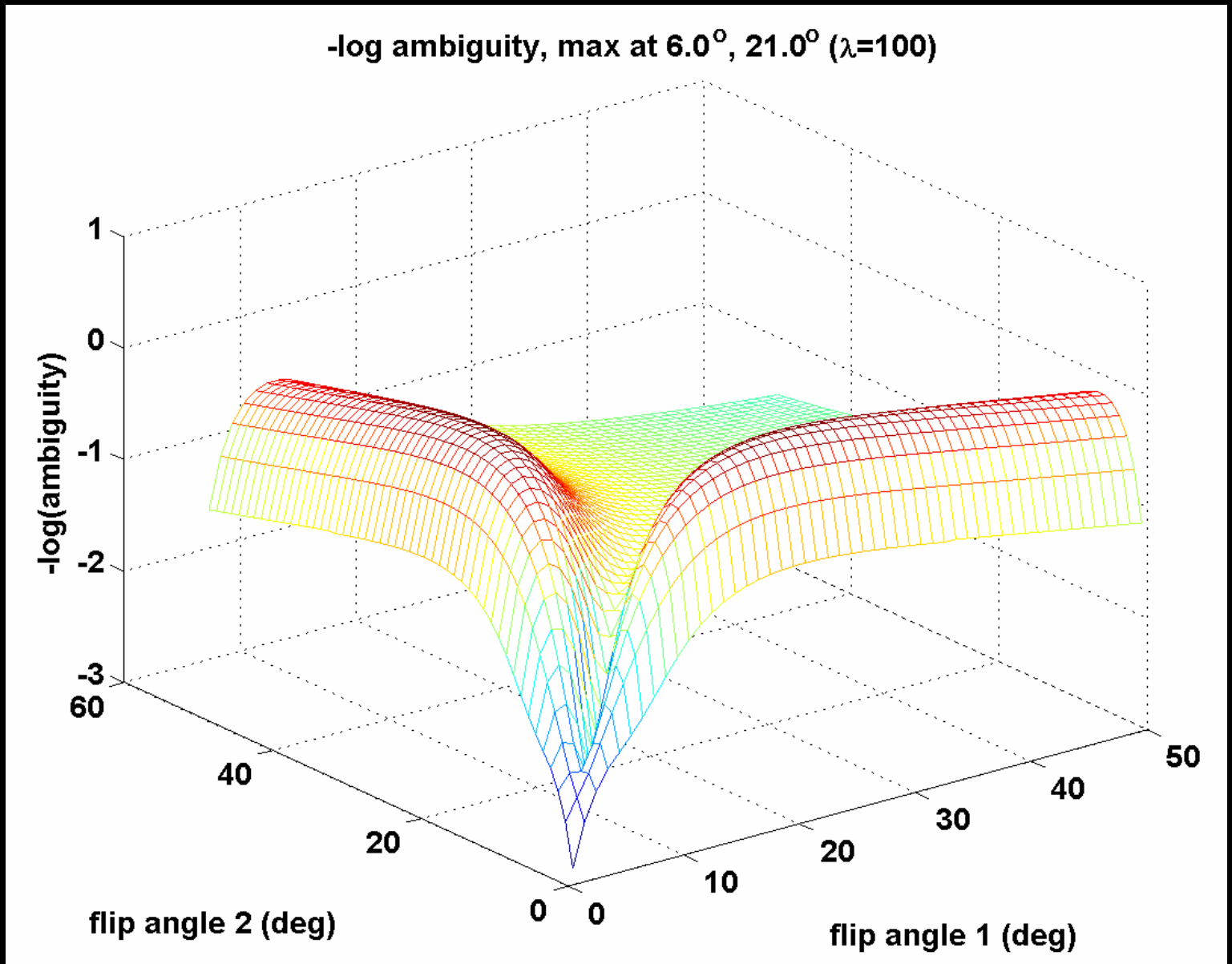

Multi-Echo Flash
(Andre van der Kouwe and Anders Dale)

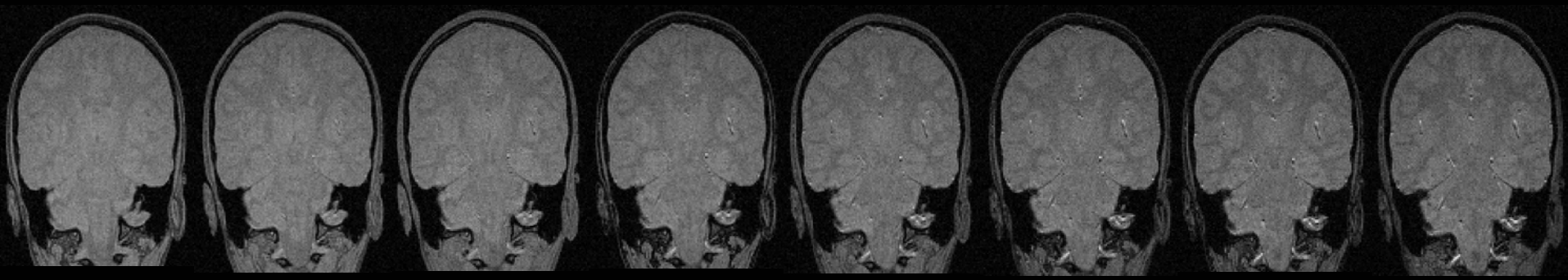

TR=20 msec, 2ms esp, flip angle=5^{o,} BW=651 Hz/voxel

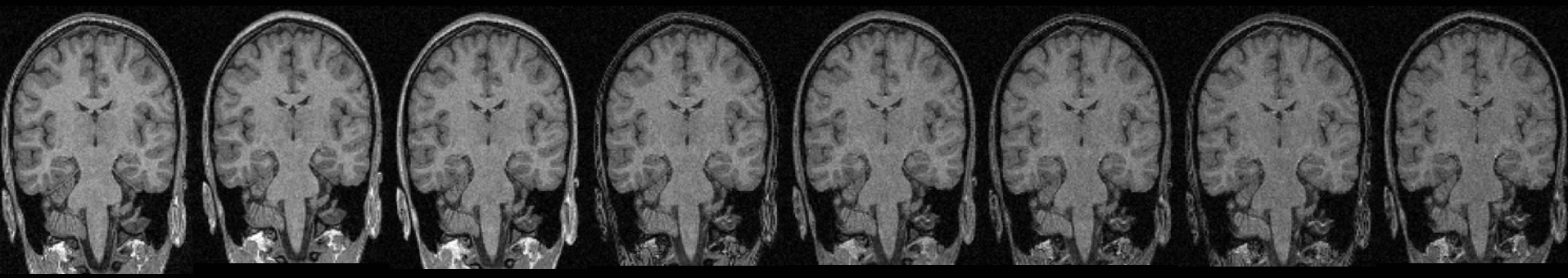

TR=20 msec, flip angle=30^{o,} BW=651 Hz/voxel

T2* decay at 5^0 (left) and 30^0 (right)

5^0 30^0

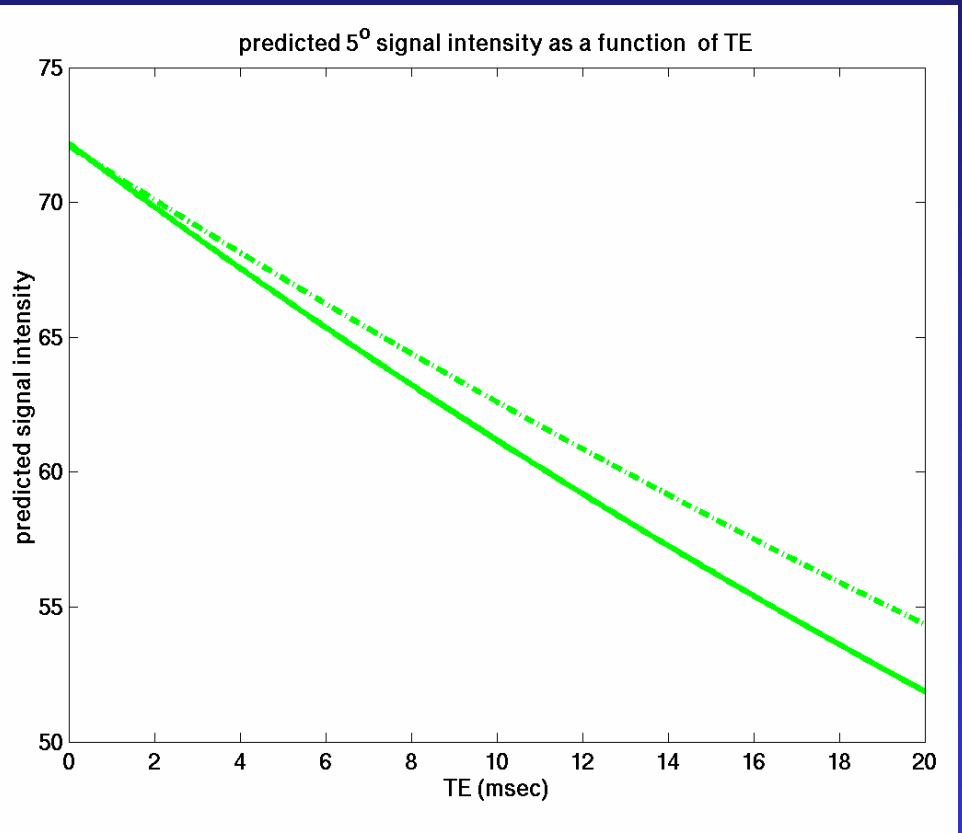

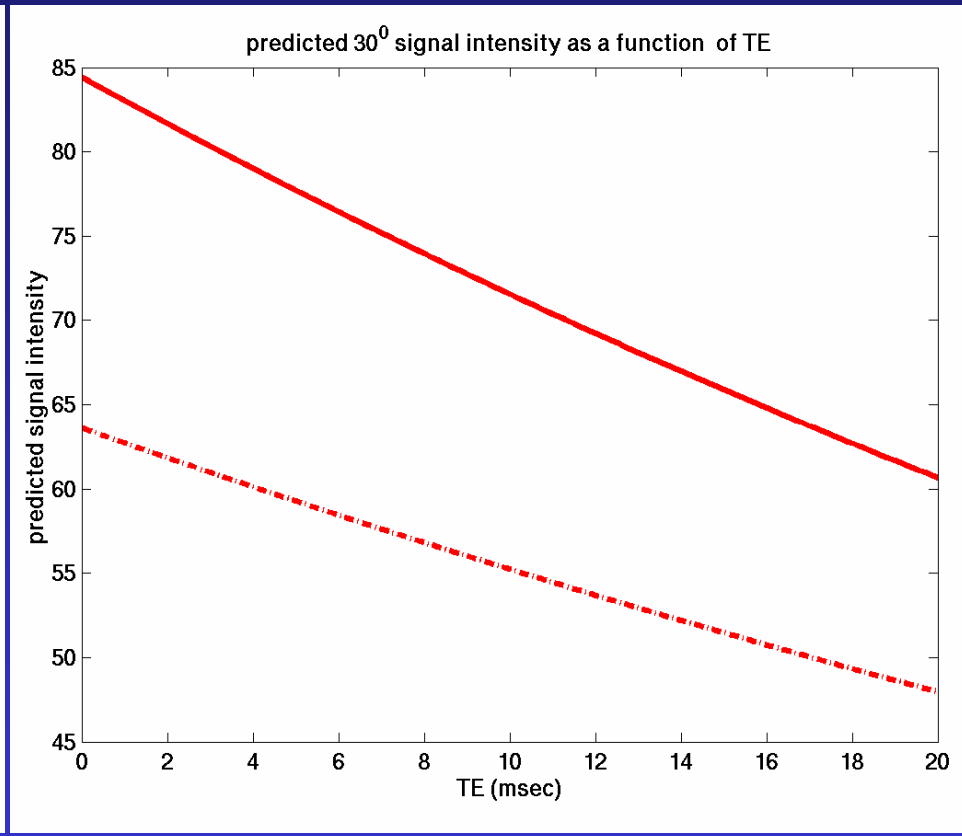

FLASH Simulation, TR=20ms, TE=3ms

GM T2*≈75 ms (dotted), WM T2*≈55 ms (solid)

T2* Decay with Echo Time
(5° left, 30° right, 65ms echo train)

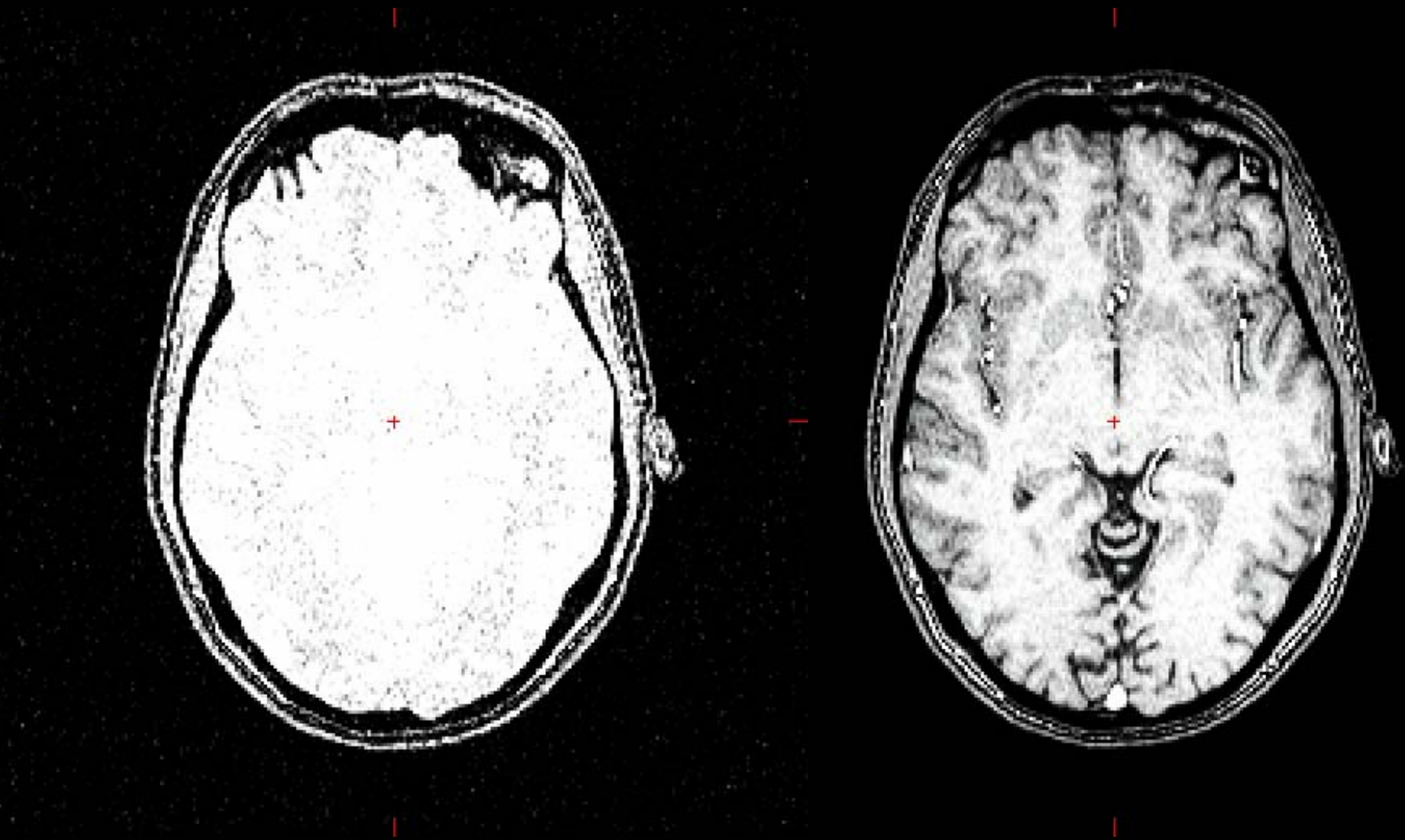

Talk Outline

1. Cortical Analysis.
2. Subcortical Analysis.
3. Sources of Variance in MRI.
4. Linking macro and microstructure.

Talk Outline

1. Cortical Analysis.
2. Subcortical Analysis.
3. Sources of Variance in MRI.
4. Linking macro and microstructure.

Sources of Variance in MRI

1. Slice positioning
2. Subject motion
3. MRI distortions
   - Gradient Nonlinearities
   - Bias fields
   - Susceptibility effects
4. Hardware/Software changes.

Longitudinal Analysis (baseline)

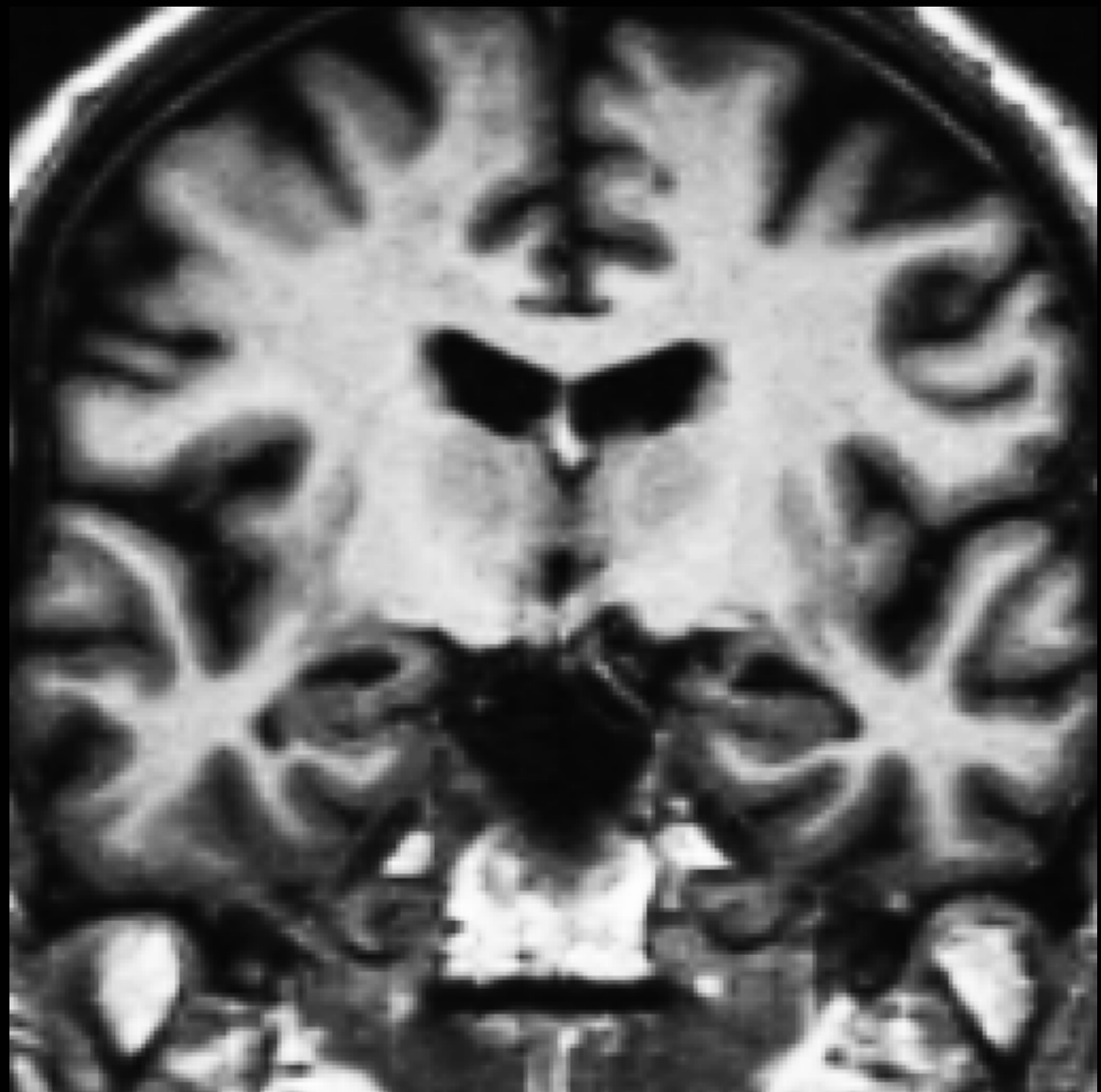

Longitudinal Analysis (600 days)

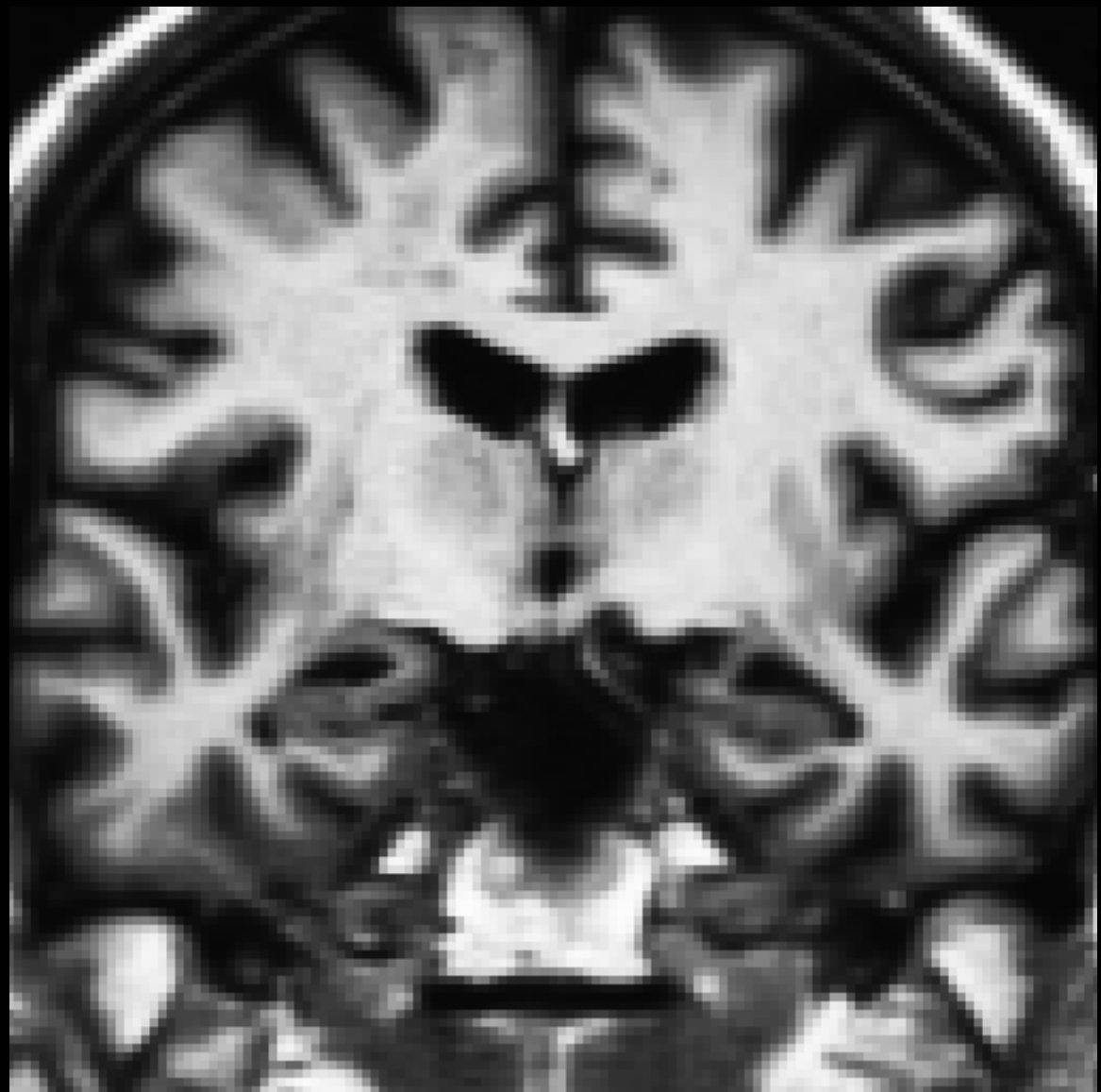

Auto Slice Registration:

prescribing where slices should be placed without human intervention

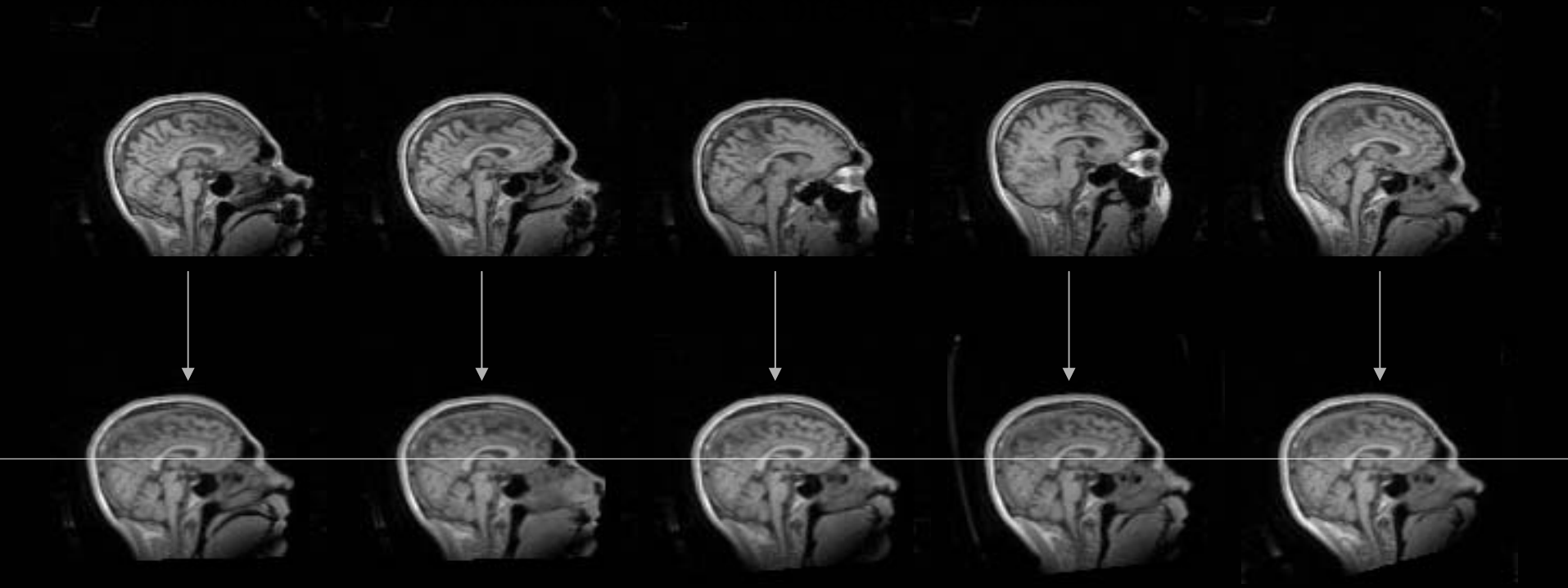

Dale / Van der Kouwe / Schmitt
MGH / Cortechs / Siemens

Real-Time Motion Correction with Cloverleaf Navigators

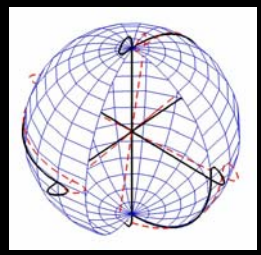

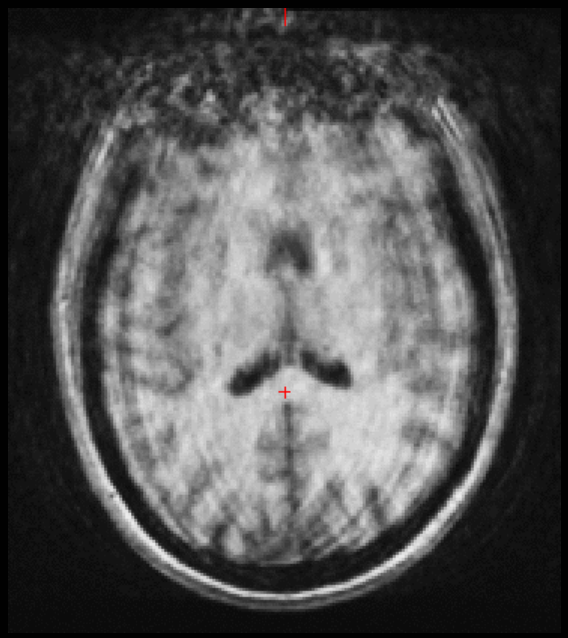

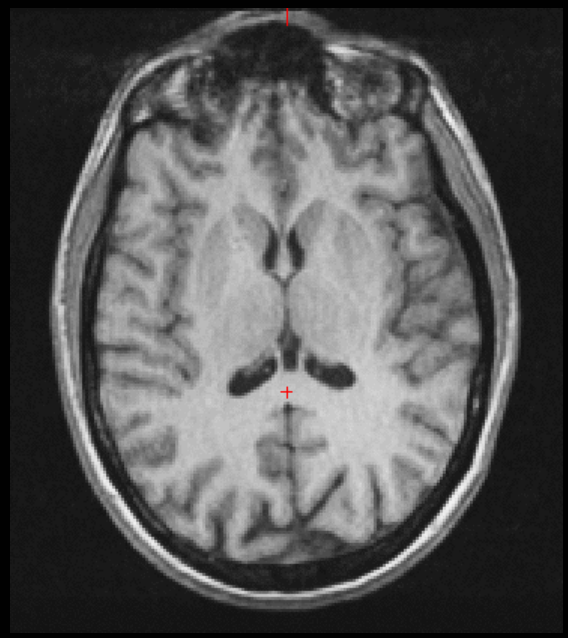

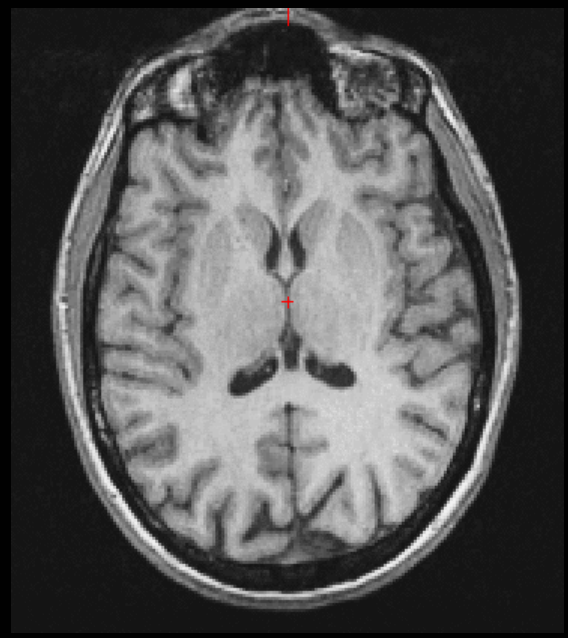

Average
No motion correction

Average (equal weight)
Real-time motion corr.

Average (MSE weighted)
Real-time motion corr.

Thanks to Andre van der Kouwe for this slide.

Gradient Distortions: Between Scanner Variance Without Correction (Scanner A)

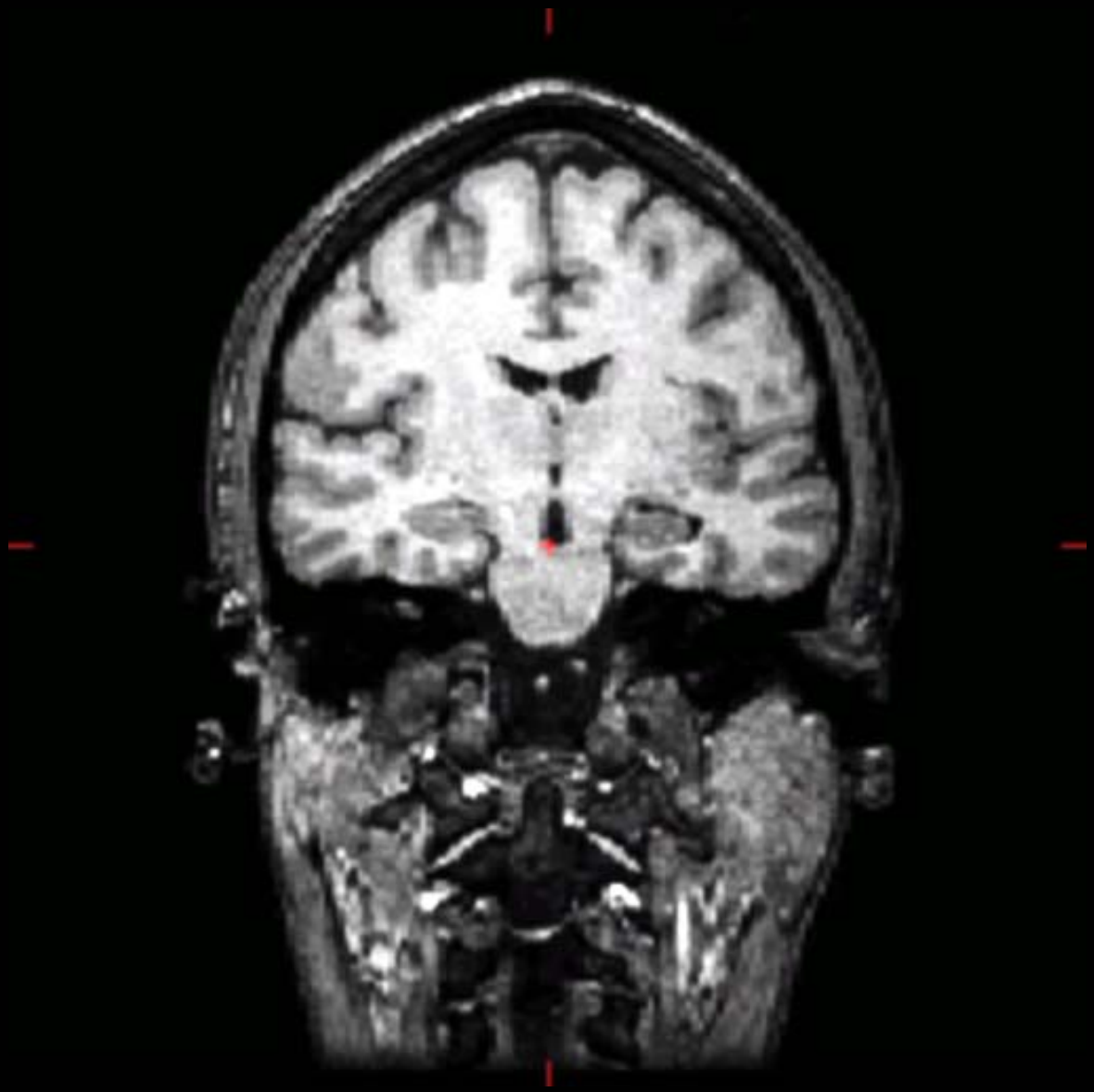

Brain Morphometry BIRN: MGH, BWH, Duke, UCSD, UCI, UCLA,JHU

Gradient Distortions: Between Scanner Variance Without Correction (Scanner B)

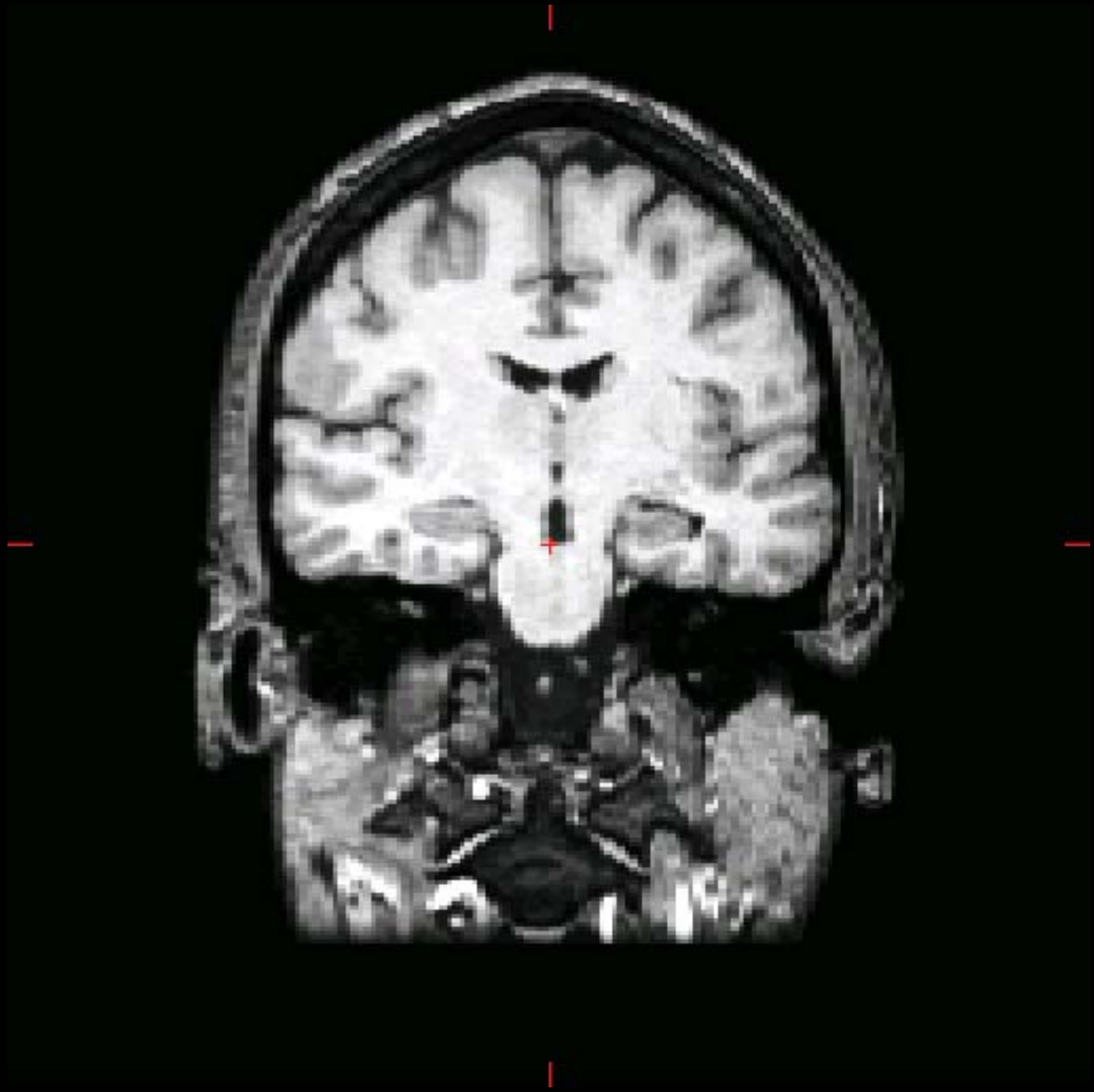

Brain Morphometry BIRN: MGH, BWH, Duke, UCSD, UCI, UCLA,JHU

Spatial Distortion due to Magnetic Susceptibility (B_0) Pulse-Sequence Dependence (S/I readout direction)

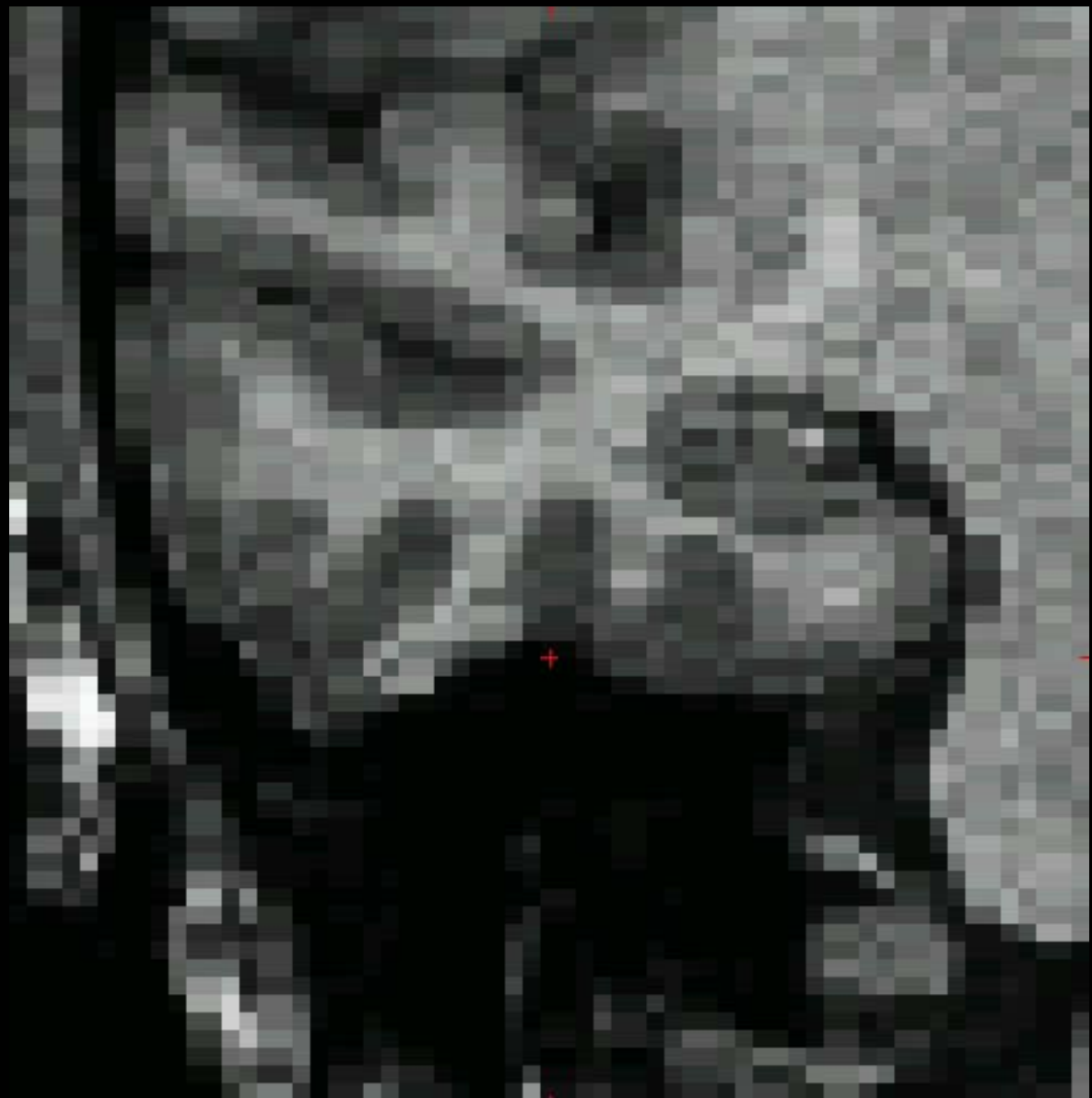

Spatial Distortion due to Magnetic Susceptibility (B_0)
Pulse-Sequence Dependence (I/S readout direction)

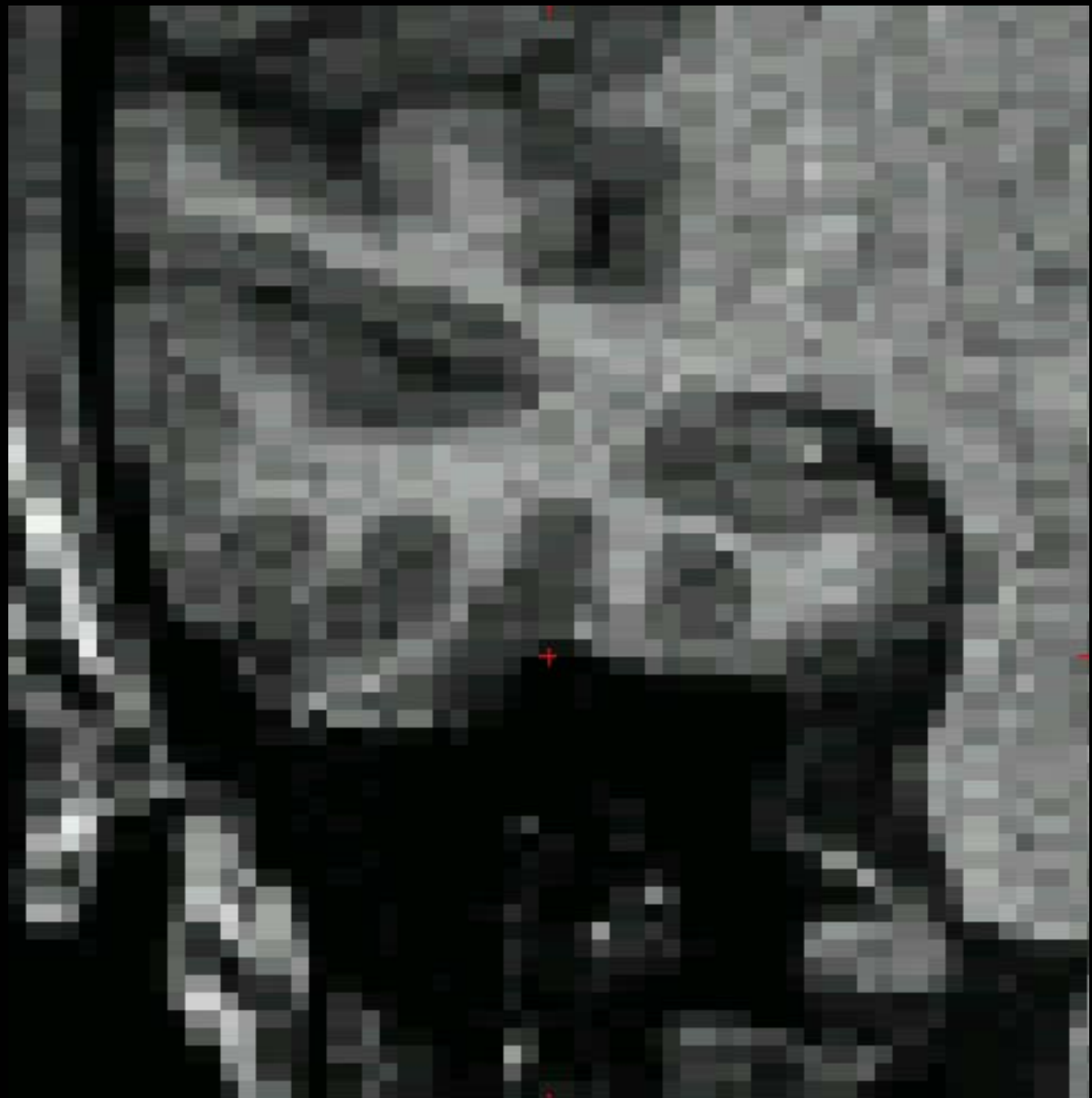

Talk Outline

1. Cortical Analysis.
2. Subcortical Analysis.
3. Sources of distortion in MRI.
4. Linking micro structure to macro structure.

Talk Outline

1. Cortical Analysis.
2. Subcortical Analysis.
3. Sources of distortion in MRI.
4. Linking micro structure to macro structure.

Histology in Alzheimer's disease

CONTROL

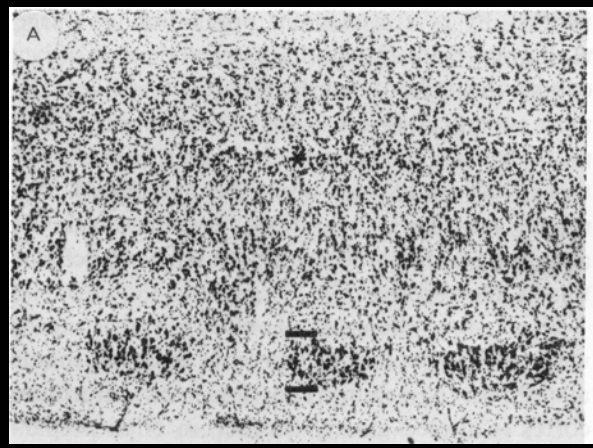

AD

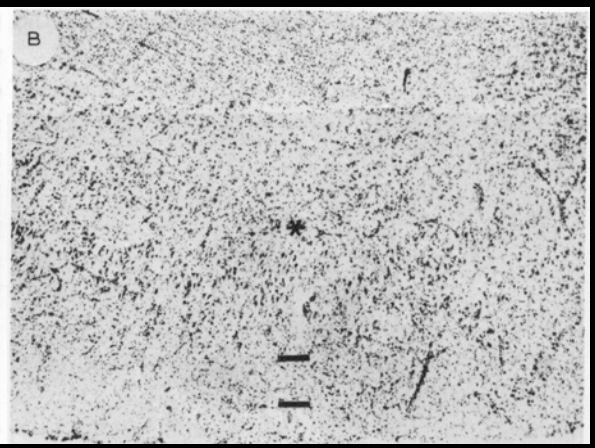

Nissl Stain

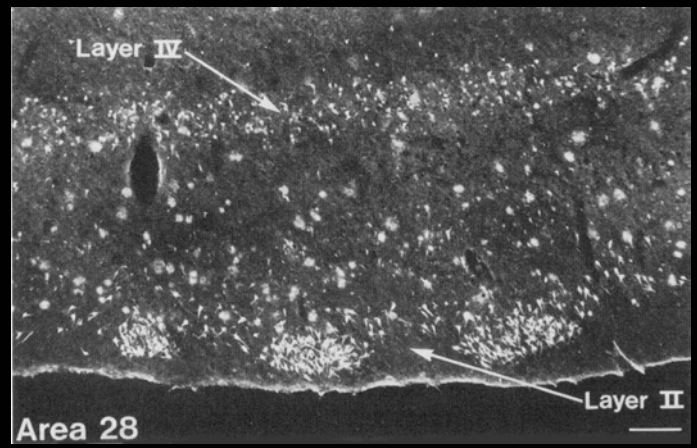

thioflavin S
(neurofibrillary tangles
and neuritic plaques)

Thanks to Brad Hyman and Jean Augustinack for this slide.

Temporal Lobe Fly-Through

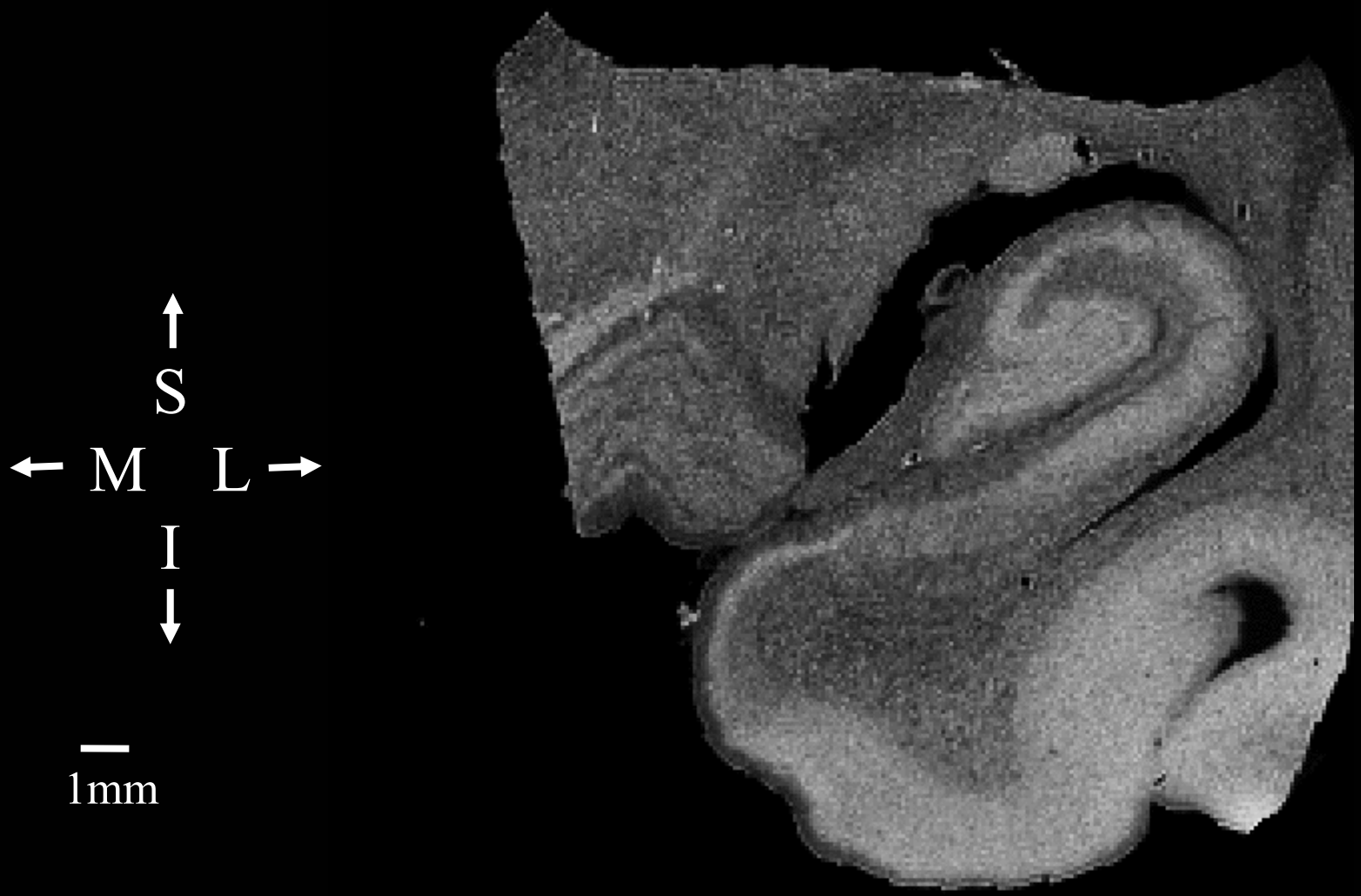

100μm isotropic MR, 7T, TR=20msec, TE=7.8msec, α=23° (synthesized)

Entorhinal Islands with MRI!

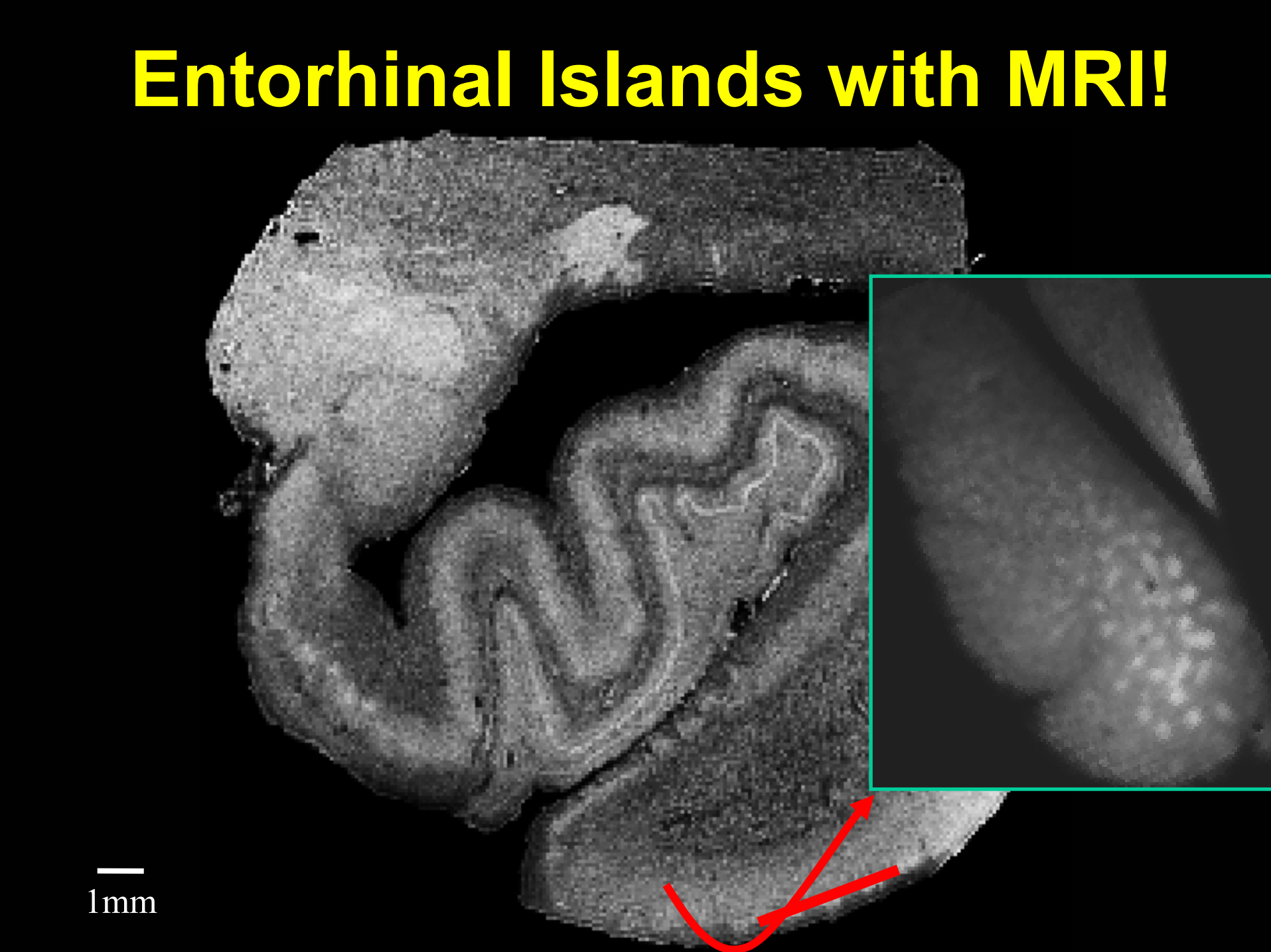

Areal border detection

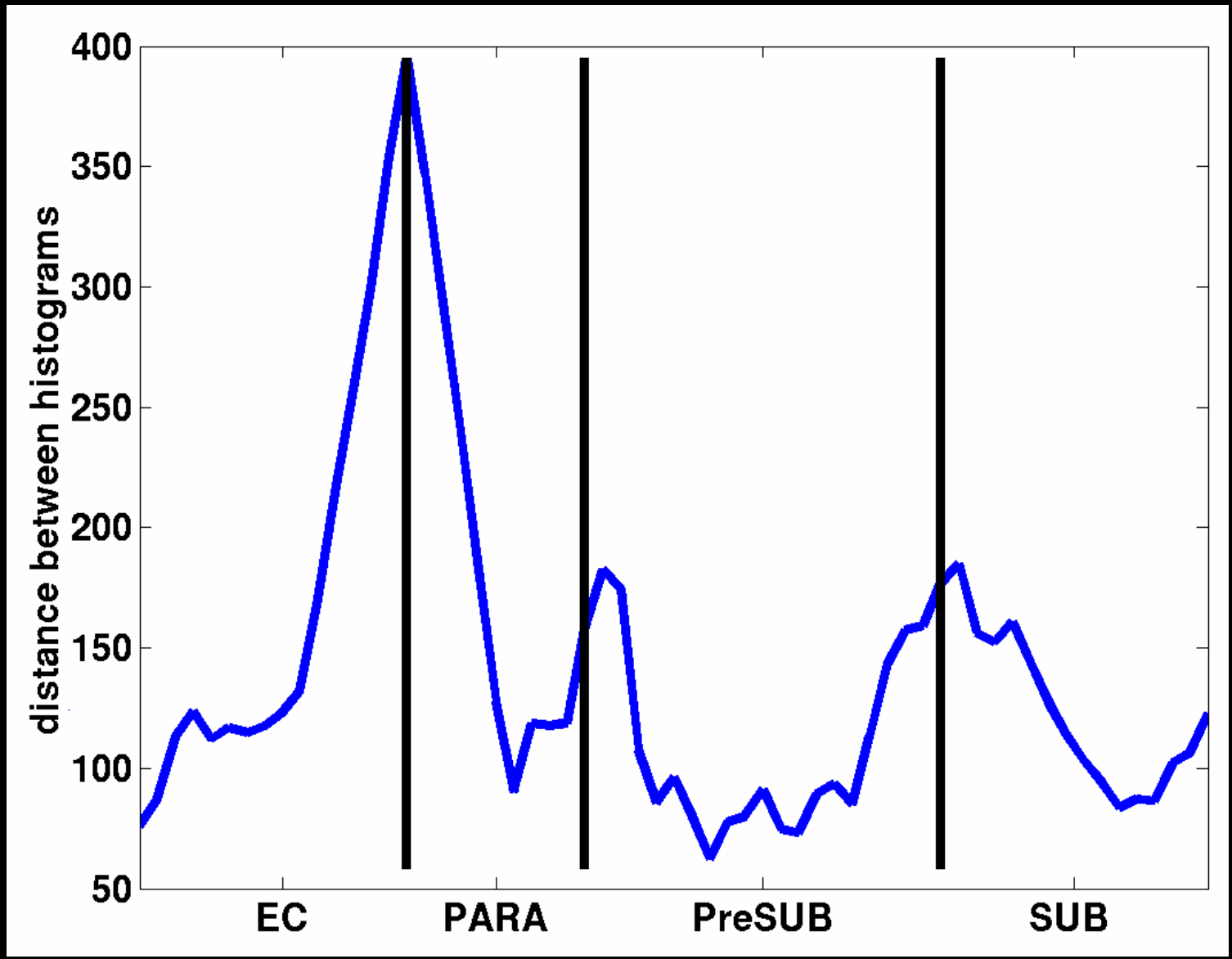

c.f. (Schleicher et al, 1999)

Towards MR Histology and Stereology

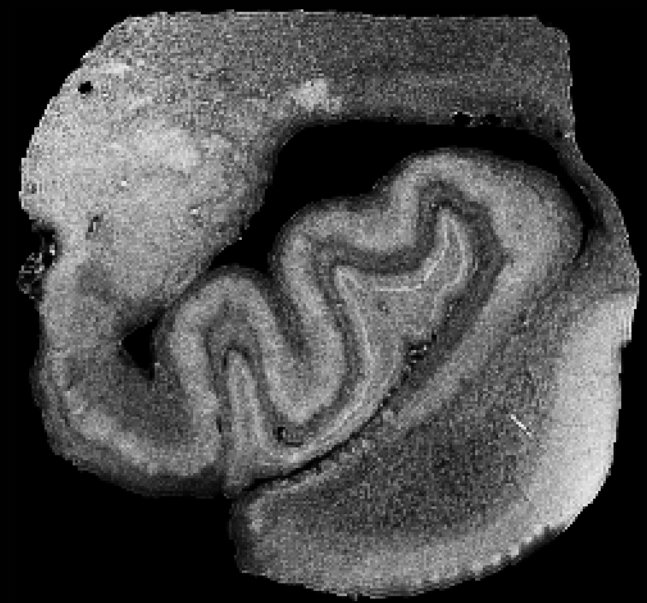

MRI

Block Face

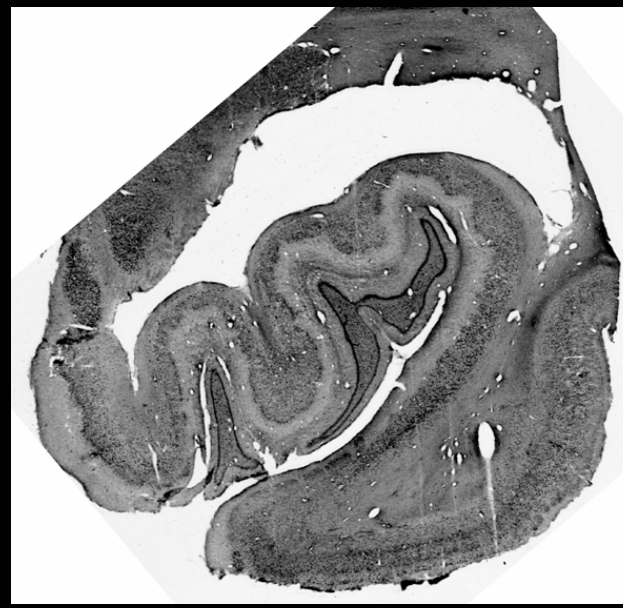

Nissl Stain

Joint work with Jean Augustinack, Larry Wald, Matt Frosch, Megan Blackwell, Chris Wiggins, David Salat and Andre van der Kouwe

Probabilistic Atlas of Cytoarchitectonic Boundaries (EC)

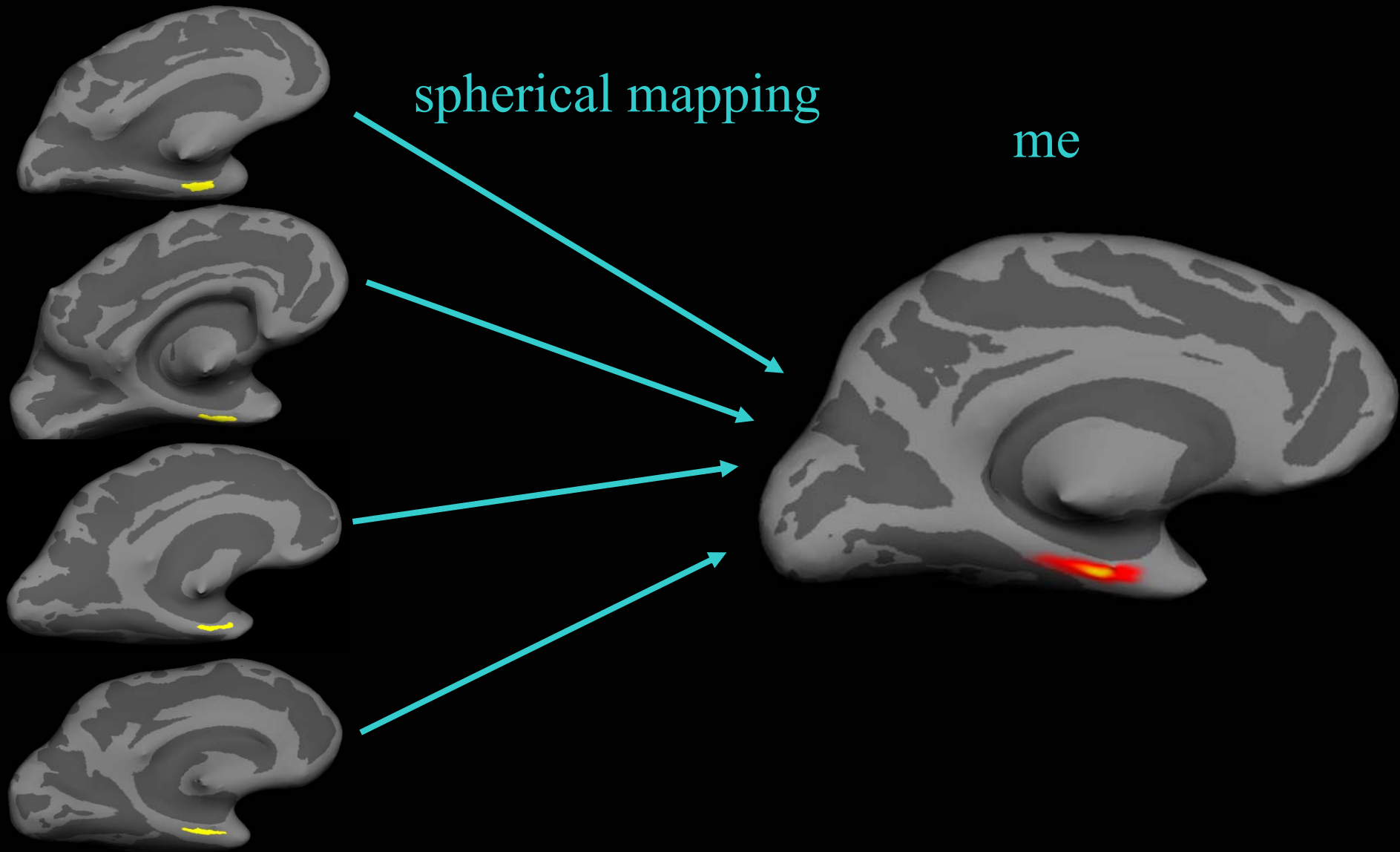

Using In-vivo Functional Data to Look for Histological Boundaries

FFA probability map

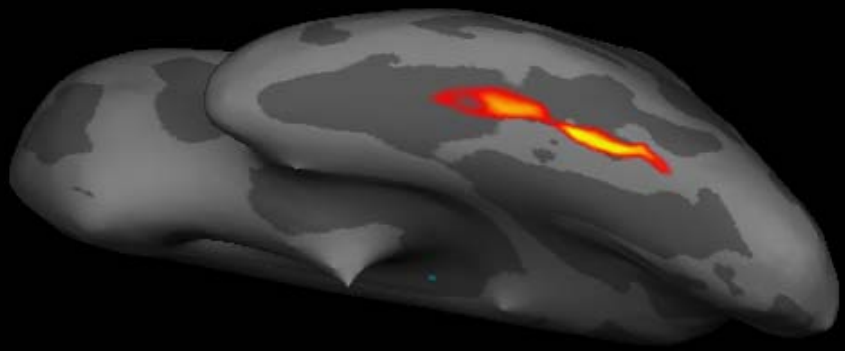

Predicted FFA border

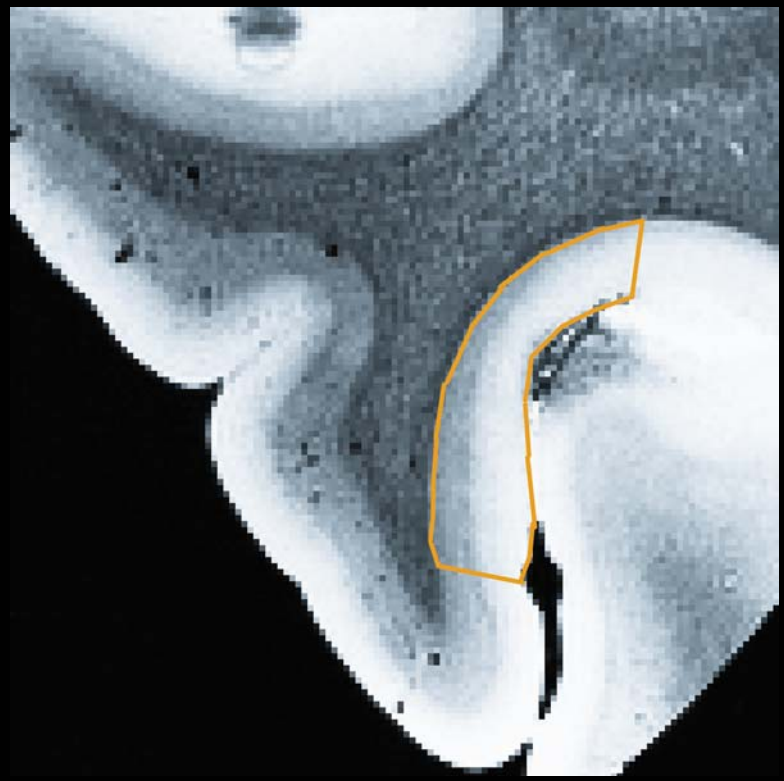

Joint work with Mona Spiridon, Nancy Kanwisher, Jean Augustinack, Becca Schwarzlose, Megan Blackwell and Brian T. Quinn.

Acknowledgements & Disclosures

MGH

Andre van der Kouwe
David Salat
Stephan Heckers
Diana Rosas
Larry Wald
Graham Wiggins
Jorge Jovicich
David Kennedy
Chris Wiggins
Nikos Makris
Megan Blackwell
Jean Augustinack

UC San Diego

Anders Dale
Marty Sereno

Johns Hopkins University

Marilyn Albert

Washington University

Randy Buckner

Siemens Medical Systems

Franz Schmitt

Cortechs Labs, Inc

Gen-Nan Chen
Mukund Balasubramanian

Georgetown University

Tom Zeffiro
Guinevere Eden
Peter E. Turkeltaub

MIT

Florent Ségonne
Polina Golland
Peng Yu
Nancy Kanwisher
Mona Spiridon

National Center for Research Resources

NATIONAL FOUNDATION FOR Functional Brain Imaging